Available online at www.sciencedirect.com
SCIENCE DIRECT
Dyes and Pigments 73 (2007) 141–161
DYES and PIGMENTS
www.elsevier.com/locate/dyepig

A semiempirical molecular orbital study of the photo-reactivity of monoazo reactive dyes derived from γ- and J-acids

Toshio Hihara [a,*], Yasuyo Okada [b], Zenzo Morita [c]

[a] Technical Center, DyStar Japan Ltd., Azuchi-machi 1-7-20, Chuo-ku, Osaka 541-0052, Japan
[b] School of Domestic Science, Otsuma Women's University, Sanban-cho, Chiyoda-ku, Tokyo 102-8357, Japan
[c] Tokyo University of Agriculture and Technology, Koganei, Tokyo 184-8588, Japan

Received 30 June 2005; accepted 7 November 2005
Available online 9 January 2006

Abstract

The reactivities (k_0: the second-order rate constants of the reaction against singlet oxygen) of 11 reactive azo dyes derived from J-acid, L-acid, R-acid, 2R-acid and γ-acid on cellulose film immersed in an aerobic aqueous Rose Bengal solution and exposed to a carbon arc were estimated and analyzed in terms of frontier orbital theory using the semiempirical molecular orbital (MO) PM5 method. The azo–hydrazone tautomerism (AHT) was analyzed by calculating the standard enthalpies of formation for these dyes in the gas phase and water using the PM5 method. If a dye existed as the same tautomer in both the gas phase and water, it was regarded to exist as that tautomer on water-swollen cellulose; if it existed as different tautomers in the gas phase and water, it was regarded to exist as a mixture of tautomers on water-swollen cellulose. The k_0 values were confirmed to correlate to the electrophilic frontier density ($f_r^{(E)}$) of the tautomer on cellulose. The sum of $f_r^{(E)}$ for the positions of reaction was confirmed to correlate linearly to $\log k_0$, although the correlation lines for the 11 dyes differed from the correlation lines reported previously for pyrazolinylazo and azobenzene dyes.
© 2005 Elsevier Ltd. All rights reserved.

Keywords: Reactive dye; Azo dyes from γ-acid and J-acid; PM5 method; Electrophilic frontier density; Reaction with singlet oxygen; Ene reaction; [2 + 2] Cycloaddition

1. Introduction

Molecular orbital (MO) theory plays a central role in our understanding of all aspects of chemical reactivity, not just the possibility or otherwise of pericyclic reactions [1–3]. Quantitative structure–activity relationships (QSAR) and quantitative structure–property relationships (QSPR) based on MO theory have been widely applied to drug design, but not to dye chemistry [4–6]. We applied frontier orbital theory to analyze the reactivity of azo dyes toward singlet molecular oxygen or bleaching agents [7,8], in addition to AHT analysis [8,9].

In a previous paper [10], we estimated three potential properties, photo-oxidizing ability (k_0: the ease with which the dye is oxidized by $^1O_2$), photosensitivity (f: the quantum yield of $^1O_2$), and photo-reductivity (relative initial rate of photo-reduction upon immersion in anaerobic DL-mandelate solution), for 15 reactive monoazo dyes using dyed cellulose films, and analyzed the photo-fading of reactively dyed cotton fabric in terms of these three potential properties in order to elucidate the photo-fading mechanism on exposure in the presence of substrates. In previous works [11,12], the photo-oxidation, or the reaction with $^1O_2$, of several yellow pyrazolinylazo and azobenzene dyes was examined using dyed cellophane films, and the positions of reaction and the corresponding reactivities of both tautomers were analyzed using the PM5 method. The reactivity of the predominant tautomers toward $^1O_2$ in the gas phase was analyzed in terms of frontier orbital theory.

In the present paper, we carry out MO calculations (PM5 method) to find the correlations between the k_0 values obtained in the previous paper [10] and newly discovered electrophilic reaction parameters at the double bonds to which singlet oxygen is added.

* Corresponding author. Tel.: +81 6 6263 6681; fax: +81 6 6263 6697.
E-mail address: hihara.toshio@DyStar.com (T. Hihara).

0143-7208/$ - see front matter © 2005 Elsevier Ltd. All rights reserved.
doi:10.1016/j.dyepig.2005.11.002

2. Experimental

2.1. Dyes used

Eleven vinylsulfonyl (VS) dyes and a monochlorotriazinyl (MCT) reactive dye derived from J-acid (two), L-acid (one), 2R-acid (one), NW-acid (one) and γ-acid (six) were used. Some of the dyes used in this study were the same as those used previously [10], whereas others were newly added. The chemical structure (the completely hydrolyzed form) of the azo tautomer of each dye, its C.I. generic name (abbreviation in parentheses), and C.I. constitution number, if available, are shown below.

(1) An orange dye derived from J-acid having a VS reactive group and an MCT bridge group (Orange JVS)

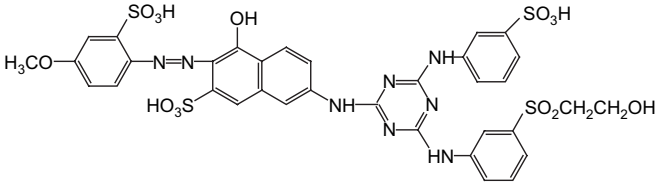

(2) C.I. Reactive Orange 7 (Orange 7), C.I. 17756

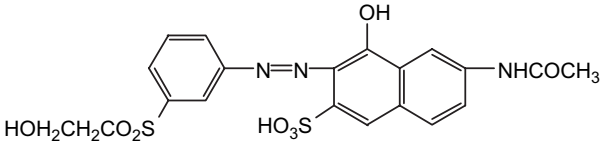

(3) C.I. Reactive Orange 16 (Orange 16), C.I. 17757

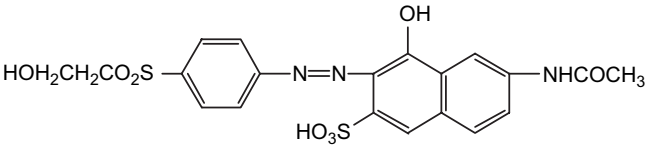

(4) C.I. Reactive Orange 72 (Orange 72), C.I. 17754

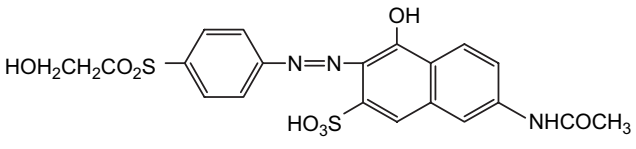

(5) C.I. Reactive Red 22 (Red 22), C.I. 14824

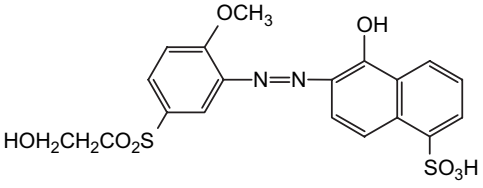

(6) A red VS dye derived from NW-acid (Red NW)

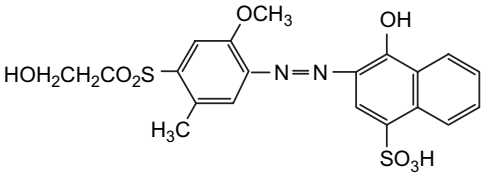

(7) A red dye derived from γ-acid having a VS group (Red gVS)

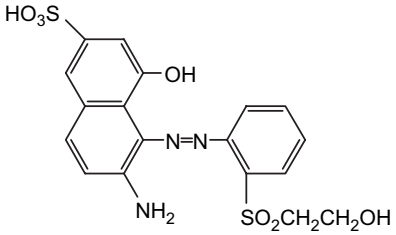

(8) A red dye derived from γ-acid having a 1-methoxy-4-VS-phenylazo group (Red mgVS)

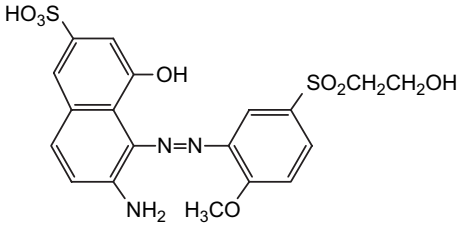

(9) A red dye derived from γ-acid having a *p*-(VS)-phenyl-azo group (Red pgVS)

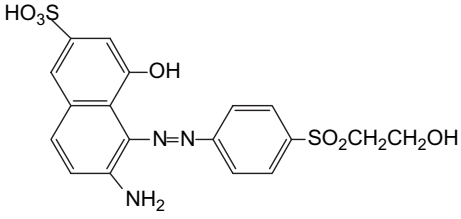

(10) A red dye derived from γ-acid having a 2-(*o*-sulfo-phenyl)-4-hydroxytriazinyl group (Red gTri)

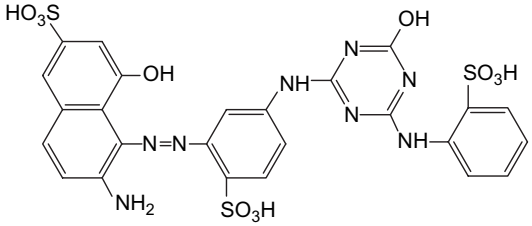

(11) A red dye derived from 2R-acid (Red 2RVS)

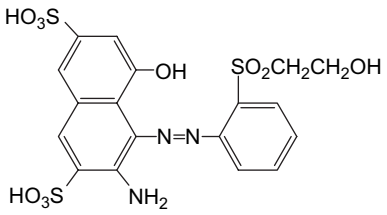

2.2. Dyeing of cellophane sheet and estimation of k_0

Cellophane films (Futamura Kagaku Kogyo K.K. #300) were dyed with each dye by alkali-shock method to obtain the absorbance between 0.4 and 0.8 at the λ_{max} by the same method as reported in previous papers [10,13]. The fading of individual dyes was estimated by exposing cellophane films dyed with reactive dyes to a carbon arc on immersing the dyed film in an aerated aqueous Rose Bengal (RB) solution. From the initial rates of relative fading, A/A_0, where A_0 and A were the absorbances measured at the λ_{max} of each dye on the initial and exposed samples, respectively, the ease with which the dye was photo-oxidized was estimated as the value of k_0 ($dm^3\ mol^{-1}\ s^{-1}$) [10,13].

2.3. Semiempirical molecular orbital calculation of the dye properties

All the MO calculations were carried out using CAChe MOPAC 2002 (Windows edition, Version 6.1.12.33.) (Fujitsu, Ltd.). For both tautomers of the 11 dyes in the gas phase and water, structure optimization was performed using the PM5 method in order to obtain some of their molecular parameters, such as the standard heat of formation ($kcal\ mol^{-1}$), electron densities in the HOMO and LUMO, electrophilic frontier densities and dipole moment. On this occasion, the van der Waals radius of water was modified from 0.1 nm to 0.13 nm.

3. Results and discussion

3.1. Ease with which the dyes are photo-oxidized by singlet oxygen

As a measure of the ease with which the dyes are photo-oxidized, the second-order rate constants, k_0 ($dm^3\ mol^{-1}\ s^{-1}$), of the reactions between each of the 11 dyes and singlet oxygen were determined from the rates of fading at the initial time of exposure of the cellulose films immersed in aqueous RB solution, by the same method used in the previous studies [13–20]. The fact that RB generates only $^1O_2$ and that the formation of superoxide is a very inefficient process has been recently reconfirmed [21,22]. The k_0 values obtained are listed in Table 1.

As a result, therefore, some reactive azo dyes were demonstrated to undergo only the photo-oxidation by $^1O_2$ on exposing the dyed cellophane immersed in an aerobic aqueous RB solution [13–16]. The fading of Pyr-Yellow on cellophane immersed in aerated water was considerably suppressed by the addition of 1,4-diazabicyclo [2.2.2] octane (Dabco) and promoted in aerated deuterium oxide [16]. A decrease in the concentration of oxygen in the aqueous solution promoted the reduction, while the increase suppressed it [17–20]. (As the extension of the effect of oxygen, it was confirmed that the photo-reduction of some dyes was promoted on dry cellophane, the simultaneous oxidative and reductive fading being observed, although the total fading was considerably decreased compared with the fading under wet conditions [17]. The photo-reduction of MCT azo dyes on dry cellophane was also observed [23].)

Using the same procedures as before [11,12], the k_0 values were also analyzed in terms of frontier orbital theory.

Table 1
Values of the rate constant, k_0 ($dm^3\ mol^{-1}\ s^{-1}$), of the second-order reaction with $^1O_2$ estimated from the initial slope of relative fading, A/A_0, for red and yellow reactive dyes on cellulose immersed in aerated Rose Bengal (3.3×10^{-5} M + 0.5 M Na_2SO_4) solution on exposure to carbon arc without filter, and the observation of the absorption spectra of decomposition products attached to cellulose

No	Red dyes	k_0	Absorption spectra of decomposed products on cellulose
1	Orange JVS	1.1_7	AB[b] similar to Red gTri, Yellow 2 [10] and Pyridone [11]
2	Orange 7[a]	0.39_1	AB particular to this dye
3	Orange 16[a]	0.19_3	AB similar to Red pgVS and Orange 72
4	Orange 72[a]	0.23_6	AB similar to Red pgVS and Orange 16
5	Red 22[a]	1.4_6	AB similar to Yellow 14 [10], Pyr-Yellow [10] and Red mgVS
6	Red NW	0.86_3	AB particular to this dye
7	Red gVS	2.6_8	AB similar to Red 2RVS
8	Red pgVS	2.3_5	AB similar to Orange 16 and Orange 72
9	Red mgVS	1.8_3	AB similar to Red 22, Yellow 14 [10] and Pyr-Yellow [10]
10	Red gTri	3.7_5	AB similar to Orange JVS, Yellow 2 [10] and Pyridone [11]
11	Red 2RVS	2.0_8	AB similar to Red gVS

[a] C.I. reactive generic name.
[b] AB = absorption band(s).

3.2. Absorption spectra of the decomposed products

Besides the k_0 values, other experimental data that can be used for the present analyses are the absorption spectra of the decomposed products bound to cellulose (cf. Figs. 1–4). Orange JVS has its reactive anchor group in the coupling component, while all the other dyes have it in the diazo component. Among the dyes with the anchor group in the diazo component, Red gTri has a unique structure with an MCT anchor, while the others have vinylsulfonylaniline with a methoxy group. It is known that when singlet oxygen is added to the coupling site, the main products of decomposition via diazotization are substituted phenols [23–29]. Therefore, the main components observed may be classified as follows (summary in Table 1):

(1) End products of Orange JVS
(2) End products of Red gTri
(3) *p*-(2-Hydroxyethylsulfonyl)phenol (Orange16, Orange 72 and Red pgVS)

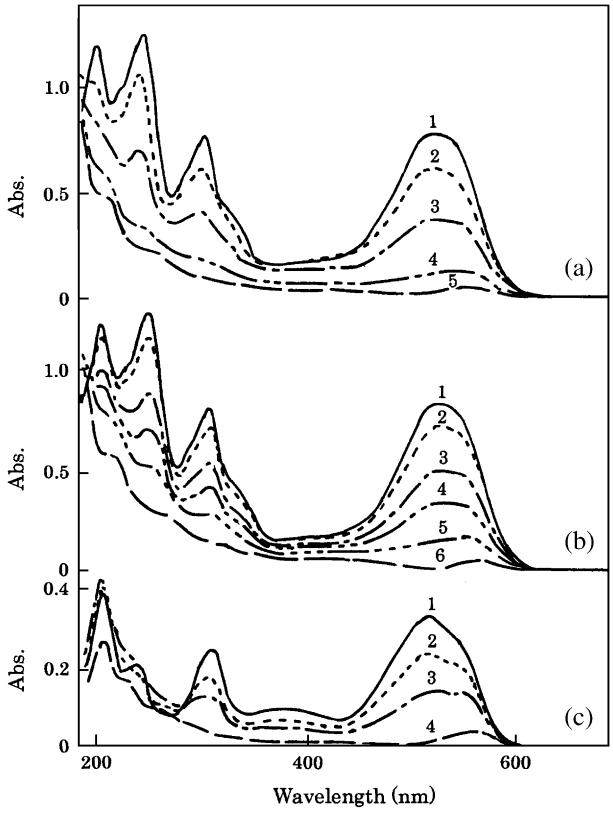

Fig. 1. Absorption spectra of the original dye (1) and of the decomposed products on cellophane film immersed in Rose Bengal solution after exposure to carbon arc for following times of exposure: (a) for Red gVS and the exposure for 15 min (2), 30 min (3), 2.5 h (4) and the calculated spectrum (5) of the decomposed products reducing that of original one from the spectrum (4), (b) for Red 2RVS and the exposure for 15 min (2), 30 min (3), 1 h (4), 2.5 h (5) and the calculated spectrum (6) of the decomposed products reducing that of original one from the spectrum (5), and (c) for Red NW and the exposure for 1 h (2), 5 h (3) and the calculated spectrum (4) of the decomposed products reducing that of original one from the spectrum (3).

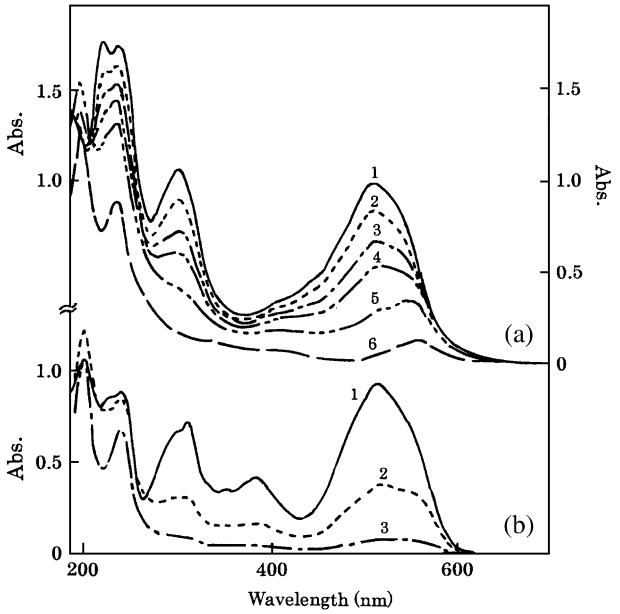

Fig. 2. Absorption spectra of the original dye (1) and of the decomposed products on cellophane film immersed in Rose Bengal solution after exposure to carbon arc for following times of exposure: (a) for mgVS and the exposure for 15 min (2), 30 min (3), 1 h (4) and 2.5 h (5) and the calculated spectrum (6) of the decomposed products reducing that of original one from the spectrum (5), and (b) for Red 22 and the exposure for 1 h (2), and 10 h (3) (completely decomposed product).

(4) *m*-(2-Hydroxyethylsulfonyl)phenol (Orange 7)
(5) *o*-(2-Hydroxyethylsulfonyl)phenol (Red gVS and Red 2RVS)
(6) *o*-Methoxy-*m*-(2-hydroxyethylsulfonyl)phenol (Red 22 and Red mgVS)
(7) End products of Red NW.

3.3. Azo–hydrazone tautomerism of azo dyes

3.3.1. AHT of the azo dyes derived from γ-acid and 2R-acid

The values of $\Delta_f H^0$(gas) and $\Delta_f H^0(H_2O)$ for these five dyes were calculated using the PM5 method, as shown in Table 2. The results indicate that azo dyes derived from 1-phenylazo-2-amino-8-naphthol-6-sulfonic acid (γ-acid) and -3,6-disulfonic acid (2R-acid) exist as azo tautomers (ATs) in both the gas phase and water, as in the case of dyes derived from 1-phenylazo-2-naphthol-6-sulfonic acid [9]. Thus, since the AHT of these dyes is very simple, only the reactivity of the ATs was investigated.

3.3.2. AHT of the azo dyes derived from acetyl-γ-acid, J-acid, NW-acid and related acids

The $\Delta_f H^0$ values calculated for both the gas phase and water showed that four dyes, Orange 7, Orange 16, Orange 72 (isomers), and Red 22 exist as hydrazone tautomers (HTs) in both phases, while the other two dyes, Orange JVS and Red NW, switched AHT during the transition from water to the gas phase (cf. Table 3). The AHT of the latter two dyes is explained in the next section.

3.4. Reactivity of azo dyes according to frontier orbital theory

$^1O_2$ allows the stereospecific and regiospecific introduction of O_2 into organic substrates. It is an electrophilic reagent with a reactivity pattern reminiscent of that exhibited by various organics, including hydroxylazo dyes and heterocycles. It undergoes [4 + 2] cycloaddition with 1,3-dienes and [2 + 2] cycloaddition and ene reactions with isolated double bonds and double bonds in aromatics [24–30]. For each reaction mode, several reaction mechanisms are known to operate, although the actual mechanism preference depends on the experimental conditions. Using the same procedure as that discussed in the previous papers [11,12], a comparison of the reactivity of the 11 phenylazo dyes examined was made in terms of frontier electron density and the sum of electrophilic frontier density (see below).

Fukui et al. [3,31–33] introduced a factor called the frontier electron density, $f_r^{(E)}$, for each electrophilic reaction type; it is the weighted sum of the squares of the coefficients

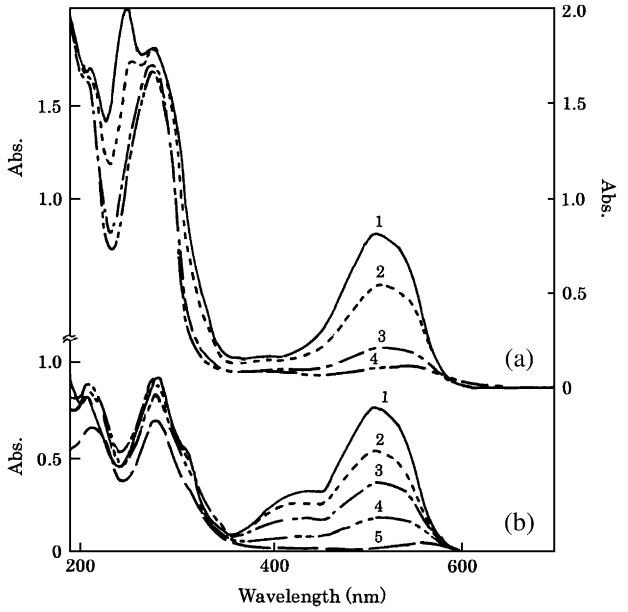

Fig. 3. Absorption spectra of the original dye (1) and of the decomposed products on cellophane film immersed in Rose Bengal solution after exposure to carbon arc for following times of exposure: (a) for gTri and the exposure for 15 min (2), 30 min (3) and 1 h (4) (completely decomposed product), and (b) for Orange JVS and the exposure for 30 min (2), 2.5 h (3) and 10 h (4) and the calculated spectrum (5) of the decomposed products reducing that of original one from the spectrum (4).

of the LCAO MO. Fukui's original expression can be written as follows:

$$f_{\mathrm{r}}^{(\mathrm{E})} = \frac{\sum_{j=1}^{N} \nu_j \left(C_r^j\right)^2 \exp\left\{-\lambda\left(E_{\mathrm{HOMO}} - E_j\right)\right\}}{\sum_{j=1}^{N} \nu_j \exp\left\{-\lambda\left(E_{\mathrm{HOMO}} - E_j\right)\right\}} \quad (1)$$

In this equation, N is the total number of orbitals, ν_j is the number of electrons in the jth orbital and is usually 0, 1, or 2, C_r^j is the coefficient of the jth LCAO MO at the rth atomic position, E_j is the energy of jth orbital, and λ is a scale factor that is usually set to 3.0 in these calculations [34].

The electrophilic reactivity of the double bonds toward $^1O_2$ may be described by the sum, $S_{m,n}^{(\mathrm{E})}$, of the $f_{\mathrm{r}}^{(\mathrm{E})}$ defined by Eq. (1) at the two adjacent atomic positions, as follows [11,12]:

$$S_{m,n}^{(\mathrm{E})} = \sum_{m,n} \left\{f_m^{(\mathrm{E})} + f_n^{(\mathrm{E})}\right\} \quad (2)$$

where m and n denote the atomic positions of the corresponding double bonds. When there is an overlap, the overlap position is counted only once, and double bonds with larger values of $\left(f_m^{(\mathrm{E})} + f_n^{(\mathrm{E})}\right)$ are taken into consideration one by one.

As in the previous studies [11,12], the predominant tautomers in the gas phase and water were determined using the PM5 method, and then the ene and [2 + 2] cycloaddition reactivities of the ATs and HTs toward $^1O_2$ were analyzed and the $S_{m,n}^{(\mathrm{E})}$ values for the two atoms of the double bond, to which $^1O_2$ may attach, were plotted against $\log k_0$, as shown in Fig. 5. According to frontier orbital theory, the

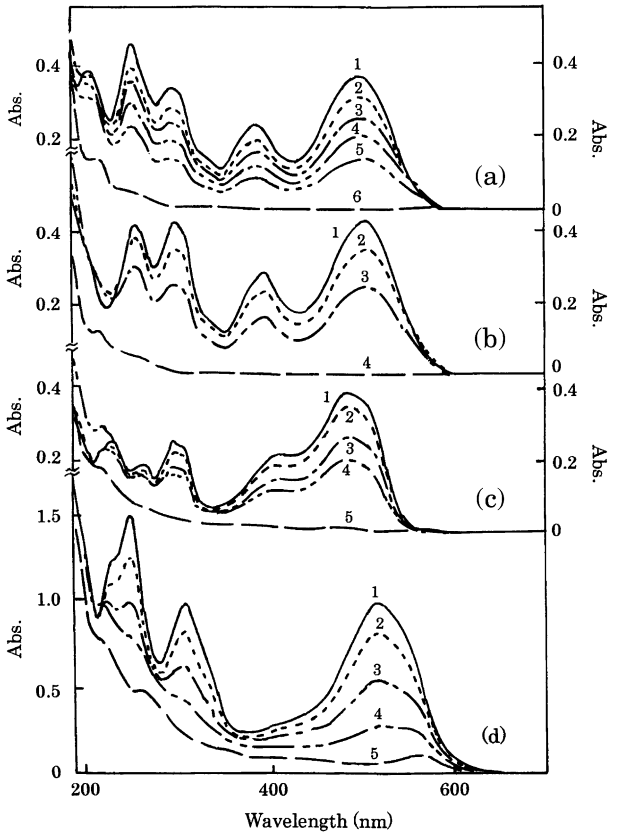

Fig. 4. Absorption spectra of the original dye (1) and of the decomposed products on cellophane film immersed in Rose Bengal solution after exposure to carbon arc for following times of exposure: (a) for Orange 7 and the exposure for 1 h (2), 2 h (3), 3 h (4), 5 h (5) and the calculated spectrum (6) of the decomposed products reducing that of original one from the spectrum (5), (b) for Orange 16 and the exposure for 2 h (2), 5 h (3) and the calculated spectrum (4) of the decomposed products reducing that of original one from the spectrum (3), (c) for Orange 72 and the exposure for 1 h (2), 3 h (3) and 5 h (4) and the calculated spectrum (5) of the decomposed products reducing that of original one from the spectrum (4), and (d) for Red pgVS and the exposure for 15 min (2), 30 min (3), 2.5 h (4) and the calculated spectrum (5) of the decomposed products reducing that of original one from the spectrum (4).

position of the reaction with $^1O_2$ is the atomic position with the largest electron density, d_{HOMO}, of the HOMO; the reactivity may be proportional to the $S_{m,n}^{(\mathrm{E})}$ values, although what reaction mode occurs as well as whether the same reaction mode occurs at the position of the second largest $S_{m,n}^{(\mathrm{E})}$ value (and one after the other) or not must be determined experimentally. The d_{HOMO} values for the 11 dyes, as calculated by the PM5 method, are listed in Tables 4 and 5. The possible reaction modes and their primary positions are summarized in Table 6. The ordinate positions ($\log k_0$) were determined or fixed experimentally, while the abscissa positions were determined so as to yield a general correlation between $\log k_0$ and the $S_{m,n}^{(\mathrm{E})}$ values.

3.5. Reaction modes of azo dyes on cellulose films

The 11 dyes were classified according to their AHT, and the reactivities of the predominant tautomers were investigated.

Table 2
Enthalpy of formation, $\Delta_f H^0$(gas) (kcal mol^{-1}), HOMO and LUMO energies, E_{HOMO} and E_{LUMO} (eV), and electrophilic frontier density, $f_r^{(E)}$, at given atoms for red azo dyes derived from γ- and 2R-acids in the gas phase, and $\Delta_f H^0$ (H_2O) (kcal mol^{-1}) in water, estimated by PM5 method

	Red gVS (gVS)		Red mgVS (mgVS)		Red pgVS (pgVS)		Red gTri (Tri)		Red 2RVS (2R)	
	451.468		481.494		451.468		704.660		531.526	
	AT	HT	AT	HT	AT	HT	AT	HT	AT	HT
$\Delta_f H^0$(gas)	−177.467	−164.665	−214.715	−206.021	−177.827	−170.155	−274.668	−259.041	−294.131	−281.121
M (debye)	8.156	7.494	5.665	8.807	7.220	5.127	10.757	10.090	9.890	9.569
E_{HOMO}	−8.850	−9.219	−8.677	−9.240	−8.872	−9.237	−8.914	−9.433	−8.859	−9.450
E_{LUMO}	−1.753	−1.893	−1.752	−1.812	−2.035	−2.135	−2.051	−1.903	−2.268	−2.374
$\Delta_f H^0$(H_2O)	−220.720	−210.686	−260.909	−250.282	−223.891	−214.484	−348.418	−331.083	−349.015	−343.120
$f_r^{(E)}$ (site)	AT		AT		AT		AT		AT	
for the most	0.462 (C1)		0.379 (C1)		0.394 (C1)		0.438 (C1)		0.534 (C1))	
probable	0.095 (C2)		0.097 (C2)		0.081 (C2)		0.061 (C2)		0.043 (C2)	
tautomer	0.083 (C8)		0.159 (C8)		0.157 (C8)		0.057 (C8)		0.071 (C8)	
	0.203 (C9)		0.226 (C9)		0.245 (C9)		0.166 (C9)		0.179 (C9)	
	0.061 (C6)		0.113 (C6)		0.119 (C6)		0.045 (C6)		0.042 (C6)	
	0.132 (C7)		0.109 (C7)		0.115 (C7)		0.113 (C7)		0.117 (C7)	
	0.089 (C5)		0.050 (C5)		0.052 (C5)		0.029 (C4)		0.101 (C14)	
	0.026 (C10)		0.038 (C10)		0.049 (C10)		0.079 (C5)		0.044 (C13)	
	0.042 (C14)						0.023 (C10)		0.062 (C18)	
	0.024 (C13)		0.029 (C14)		0.033 (C14)		0.079 (C16)			
	0.025 (C18)		0.053 (C13)		0.019 (C13)		0.018 (C17)		0.101 (C16)	
			0.031 (C18)		0.033 (C18)		0.066 (C14)		0.027 (C17)	
	0.015 (C17)		0.025 (C16)		0.036 (C16)		0.026 (C13)		0.019 (C3)	
	0.039 (C16)		0.004 (C17)		0.004 (C17)		0.055 (C18)		0.042 (C4)	
	0.028 (N11)		0.018 (C3)		0.020 (C3)				0.074 (C5)	
	0.224 (N12)		0.053 (C4)		0.044 (C4)		0.018 (N11)		0.007 (C10)	
	0.029 (C3)		0.018 (N11)		0.012 (N11)		0.251 (N12)		0.012 (N11)	
	0.045 (C4)		0.160 (N12)		0.185 (N12)				0.298 (N12)	

3.5.1. Reaction modes of the azo dyes derived from γ- and 2R-acids

The distribution of d_{HOMO} listed in Table 4 shows that almost all of the double bonds may react with singlet oxygen: C1=C2, C4=C5, C6=C7, C8=C9, C5=C10, C13=C14, C13=C18 and N11=N12. As a common feature of the ATs of the azo dyes of this series, the reactivity at C3=C4 and N11=N12 may be excluded due to the small values of d_{HOMO} at C3 (0.000−0.004) (Red 2RVS is an exception here) and that at N11 (0.000−0.001). The similarity in the reactivity of the five dyes of this group is summarized in Table 6. The reactivity of these double bonds in each dye is analyzed below.

3.5.1.1. ATs of Red gVS. The $\Delta_f H^0$(gas) values for the reaction intermediates and products were calculated by the PM5 method, and are listed in Tables 7 and 8. The order of reactivity, based on the $\Delta_f H^0$(gas) values for the reaction products, was as follows:

$$\begin{aligned}&\text{ene (C8=C9; H(O19))} > \text{[2 + 2] addition (C8=C9)} \\ &> \text{[2 + 2] addition (C3=C4)} > \text{[2 + 2] addition (C1=C2)} \\ &> \text{[2 + 2] addition (C16=C17)} \approx \text{[2 + 2] addition} \\ &\text{(C13=C14)} > \text{ene(C1=C2; H(N20))} > \text{[2 + 2] addition} \\ &\text{(C15=C16)} > \text{[2 + 2] addition (C6=C7)} > \text{[2 + 2]} \\ &\text{addition (C5=C10)} \approx \text{[2 + 2] addition (C13=C18)} \\ &\gg \text{[2 + 2] addition (N11=N12).} \end{aligned} \quad (3)$$

This order seemed to be considerably different from the order based on the $S_{m,n}^{(E)}$ values listed in Table 2. The $\Delta_f H^0$(gas) values for the reaction products underscored the reactivity of the double bond C3=C4, irrespective of the least estimated reactivity based on the $S_{m,n}^{(E)}$ values, while the $S_{m,n}^{(E)}$ values underscored that of C5=C10 irrespective of the least estimated reactivity based on the $\Delta_f H^0$(gas) value. Since the two values led to completely opposite conclusions, no reasonable explanation was possible. But since the $\Delta_f H^0$(gas) values for the reaction intermediates at Transition State Geometry (TSG) had a narrow range, inequality (3) was considered to be unimportant. As in the previous studies [10,11], the reactivity against $^1O_2$ was investigated based on the $S_{m,n}^{(E)}$ values. Among the double bonds with potential reactivity, the double bonds that contributed to the reactivities mentioned above were first clarified. Then, the plot of $S_{m,n}^{(E)}(m,n: 1,2; 5-10; 13, 14,$ and $18)$ against $\log k_0$ was found to show a good coincidence with the common correlation line, which was constructed from the plots for all the dyes examined. The contribution of the double bonds C16=C17, N11=N12 and C3=C4, which are listed in the lower part of Table 2, may be excluded due to the small d_{HOMO} values at C17 (0.005), N11 (0.001) and C3 (0.003), despite the considerable values of $f_r^{(E)}$ (r = C16 and N11) at the other end of the double bonds [11,12]. If the contribution from C16=C17 and/or N11=N12 is added to the $S_{m,n}^{(E)}(m,n)$ value, the plots deviate from the correlation line in the direction of higher reactivity, indicating that the double bonds C16=C17 and N11=N12

Table 3
Enthalpy of formation, $\Delta_f H^0$ (kcal mol^{-1}), HOMO and LUMO energies, E_{HOMO} and E_{LUMO} (eV), and electron densities of HOMO and LUMO, d_{HOMO} and d_{LUMO}, at given atoms for azo and hydrazone tautomers of azo dyes derived from H-acid and other naphthalene sulfonic acid in the gas phase, estimated by semiempirical molecular orbital PM5 method

	Orange JVS (JVS)		Orange 7 (O7)		Orange 16 (O16)		Orange 72 (O72)		Red NW (NW)		Red 22 (R22)	
M.W.	902.896		493.505		493.505		493.505		480.507		466.480	
	AT	HT	AT	HT	AT	HT	AT	HT	AT	HT	AT	HT
$\Delta_f H^0$(gas)	−354.431	−352.857	−219.706	−220.247	−220.251	−221.584	−221.211	−223.175	−215.035	−214.125	−204.674	−213.703
μ	9.071	11.489	11.285	12.253	13.023	14.349	11.143	13.352	3.989	5.344	9.603	7.280
E_{HOMO}	−9.036	−9.531	−9.044	−9.114	−9.172	−9.191	−9.163	−9.258	−9.295	−9.464	−9.008	−9.235
E_{LUMO}	−2.024	−2.169	−1.895	−2.177	−2.107	−2.266	−2.115	−2.308	−2.079	−2.017	−1.704	−1.864
$\Delta_f H^0(H_2O)$	−434.381	−439.714	−270.714	−273.645	−270.363	−275.690	−270.224	−274.907	−254.191	−257.024	−248.377	−257.091
$f_r^{(E)}$ (Site)	AT	HT	AT	HT	HT		HT		AT	HT	HT	
for the most	0.240 (C1)	0.091 (C1)	0.277 (C1)	0.243 (C1)	0.216 (C1)		0.259 (C1)		0.220 (C1)	0.113 (C4)	0.303 (C1)	
probable	0.126 (C2)	0.044 (N11)	0.219 (C2)	0.077 (N11)	0.068 (N11)		0.064 (N11)		0.096 (C2)	0.204 (C5)	0.093 (N11)	
tautomer	0.076 (C6)	0.118 (C16)	0.213 (C4)	0.083 (C9)	0.068 (C9)		0.084 (C9)		0.128 (C4)	0.160 (C1)	0.280 (C9)	
	0.121 (C7)	0.064 (C17)	0.129 (C5)	0.111 (C10)	0.099 (C10)		0.069 (C10)		0.112 (C5)	0.049 (N11)	0.127 (C10)	
	0.100 (C16)	0.075 (C14)	0.047 (C6)	0.107 (C14)	0.116 (C14)		0.116 (C14)		0.053 (C6)	0.181 (C9)	0.032 (C14)	
	0.079 (C17)	0.094 (C13)	0.117 (C7)	0.122 (C13)	0.087 (C13)		0.088 (C13)		0.157 (C7)	0.071 (C10)	0.075 (C13)	
	0.023 (C18)	0.033 (C18)	0.045 (C14)	0.064 (C18)	0.134 (C18)		0.140 (C18)		0.077 (C13)	0.095 (C3)	0.056 (C18)	
	0.101 (C13)	0.029 (C9)	0.065 (C13)	0.074 (C4)	0.065 (C4)		0.031 (C4)		0.145 (C18)	0.151 (C8)	0.075 (C3)	
	0.057 (C14)	0.046 (C10)	0.149 (C9)	0.092 (C5)	0.083 (C5)		0.051 (C5)		0.094 (C15)		0.023 (C8)	
	0.026 (C15)	0.023 (C4)	0.099 (C10)						0.079 (C16)		0.037 (C15)	
	0.084 (C4)	0.056 (C5)							0.074 (C17)	0.039 (C14)	0.031 (C16)	
	0.032 (C5)			0.029 (C15)	0.026 (C6)		0.039 (C6)			0.033 (C13)		
	0.032 (N11)		0.026 (C18)	0.106 (C16)	0.048 (C7)		0.077 (C7)			0.099 (C18)		
	0.104 (N12)	0.066 (C3)	0.011 (C15)	0.024 (C17)	0.022 (C15)		0.025 (C15)		0.043 (C14)	0.046 (C6)	0.018 (C6)	
	0.114 (C9)	0.026 (C8)	0.048 (C16)	0.016 (C3)	0.159 (C16)		0.162 (C16)		0.039 (C3)	0.176 (C7)	0.079 (C7)	
	0.034 (C10)	0.020 (C15)	0.016 (C3)	0.079 (C8)	0.016 (C17)		0.016 (C17)		0.042 (C8)	0.070 (C15)	0.103 (C5)	
		0.046 (C6)	0.051 (C8)	0.023 (C6)	0.017 (C3)		0.054 (C3)		0.198 (C9)	0.030 (C16)	0.013 (C4)	
		0.060 (C7)		0.057 (C7)	0.079 (C8)		0.021 (C8)		0.030 (C10)	0.059 (C17)		
	0.023 (C3)								0.043 (N11)			
	0.013 (C8)								0.102 (N12)			

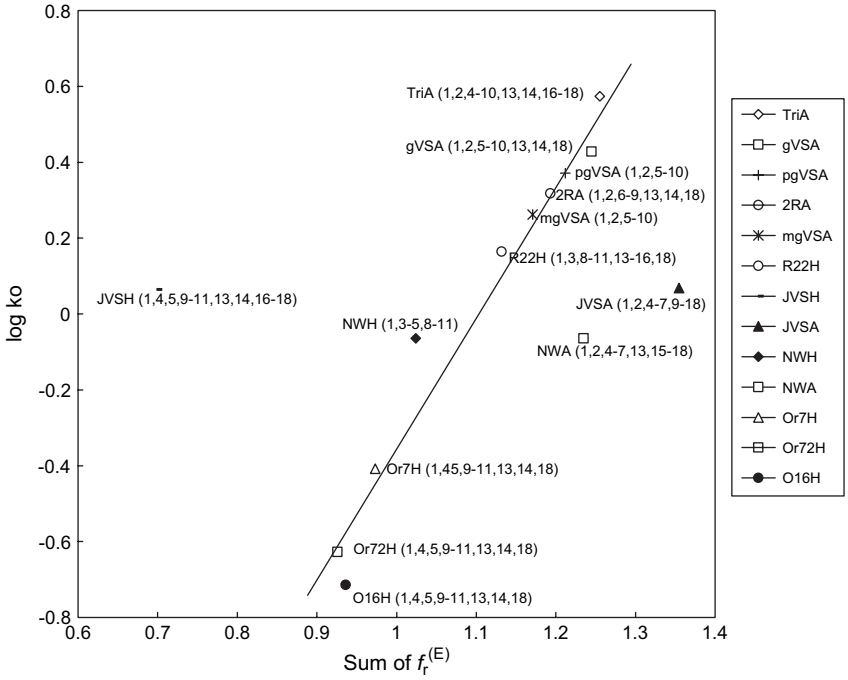

Fig. 5. Relationship between $\log k_0$ and the sum of $f_r^{(E)}$ for a series of azo dyes from γ- and J-acids.

Table 4
Electron densities at each atom in HOMO for the A&HTs of azo dyes from γ- and 2R-acids

Dye	Red gVS[a]		Red mgVS[b]		Red pgVS[c]		Red gTri[d]		Red 2RVS[e]	
	d_{HOMO}		d_{HOMO}		d_{HOMO}		d_{HOMO}		d_{HOMO}	
Tautomer	AT	HT	AT	HT	AT	HT	AT	HT	AT	HT
C1	0.263	0.139	0.211	0.091	0.217	0.121	0.264	0.032	0.279	0.133
C2	0.053	0.001	0.053	0.000	0.044	0.001	0.036	0.001	0.022	0.001
C3	0.002	0.012	0.000	0.000	0.000	0.001	0.003	0.019	0.008	0.000
C4	0.023	0.003	0.029	0.000	0.024	0.000	0.015	0.007	0.022	0.000
C5	0.037	0.020	0.015	0.000	0.014	0.006	0.037	0.023	0.036	0.004
C6	0.024	0.003	0.055	0.085	0.058	0.019	0.017	0.167	0.019	0.025
C7	0.075	0.033	0.060	0.044	0.063	0.032	0.067	0.024	0.060	0.031
C8	0.032	0.001	0.076	0.064	0.073	0.013	0.022	0.127	0.033	0.016
C9	0.108	0.041	0.122	0.144	0.132	0.064	0.092	0.175	0.091	0.070
C10	0.013	0.037	0.019	0.101	0.026	0.046	0.012	0.090	0.003	0.043
N11	0.001	0.055	0.001	0.073	0.001	0.040	0.003	0.042	0.001	0.046
N12	0.115	0.300	0.082	0.188	0.096	0.277	0.145	0.077	0.151	0.281
C13	0.007	0.041	0.022	0.013	0.007	0.042	0.011	0.006	0.020	0.044
C14	0.015	0.043	0.015	0.014	0.015	0.070	0.033	0.003	0.050	0.069
C15	0.000	0.024	0.006	0.002	0.000	0.000	0.001	0.000	0.000	0.003
C16	0.034	0.079	0.012	0.002	0.016	0.095	0.039	0.004	0.051	0.070
C17	0.005	0.002	0.000	0.002	0.000	0.000	0.009	0.001	0.013	0.023
C18	0.011	0.076	0.014	0.003	0.014	0.072	0.025	0.005	0.031	0.035
O19	0.034	0.019	0.086	0.131	0.092	0.045	0.000	0.176	0.032	0.052
N20	0.138	0.040	0.106	0.018	0.100	0.027	0.000	0.001	0.063	0.016

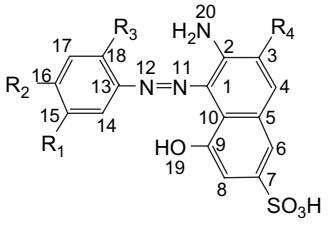

[a] Red gVS ($R_1 = R_2 = R_4 = H$, $R_3 = SO_2CH_2CH_2OH$).
[b] Red mgVS ($R_1 = SO_2CH_2CH_2OH$, $R_2 = R_4 = H$, $R_3 = OCH_3$).
[c] Red pgVS ($R_1 = R_3 = R_4 = H$, $R_2 = SO_2CH_2CH_2OH$).
[d] Red gmTriVS (R_1 = 6-hydroxy-4-(2′-sulfoanilino)-1,3,5-triazin-2-ylamino, $R_2 = R_4 = H$, $R_3 = SO_3H$).
[e] Red 2RVS ($R_1 = R_2 = H$, $R_3 = SO_2CH_2CH_2OH$, $R_4 = SO_3H$).

Table 5
Electron densities, d_{HOMO}, at each atom of azo and hydrazone tautomers for Orange JVS, C.I. Reactive Red 22, Orange 7, Orange 16 and Red NW in the gas phase, using PM5 method

	Orange JVS[a]		Orange 7[b]		Orange 16[c]		Orange 72[d]		Red 22[e]		Red NW[f]	
	AT	HT	AT	HT	AT	HT	AT	HT	AT	HT	AT	HT
C1	0.176	0.105	0.159	0.141	0.154	0.130	0.201	0.163	0.198	0.170	0.154	0.104
C2	0.091	0.001	0.134	0.005	0.125	0.004	0.093	0.006	0.136	0.009	0.068	0.004
C3	0.005	0.002	0.001	0.004	0.002	0.005	0.018	0.001	0.002	0.031	0.000	0.028
C4	0.056	0.008	0.124	0.031	0.135	0.026	0.066	0.012	0.033	0.006	0.080	0.069
C5	0.009	0.015	0.064	0.039	0.072	0.033	0.004	0.011	0.028	0.050	0.043	0.143
C6	0.049	0.000	0.012	0.002	0.009	0.002	0.078	0.002	0.011	0.004	0.028	0.001
C7	0.079	0.019	0.071	0.029	0.075	0.024	0.130	0.028	0.062	0.042	0.098	0.115
C8	0.003	0.011	0.003	0.026	0.008	0.025	0.006	0.005	0.014	0.006	0.001	0.102
C9	0.082	0.032	0.091	0.049	0.087	0.042	0.099	0.052	0.162	0.159	0.136	0.139
C10	0.015	0.038	0.051	0.058	0.059	0.053	0.017	0.037	0.014	0.067	0.002	0.051
N11	0.009	0.040	0.006	0.042	0.003	0.039	0.004	0.037	0.013	0.047	0.011	0.031
N12	0.065	0.227	0.052	0.259	0.050	0.270	0.069	0.302	0.062	0.237	0.057	0.125
C13	0.052	0.101	0.025	0.064	0.013	0.048	0.015	0.053	0.051	0.030	0.042	0.007
C14	0.034	0.080	0.019	0.056	0.014	0.058	0.016	0.061	0.022	0.015	0.003	0.003
C15	0.010	0.012	0.003	0.012	0.000	0.004	0.000	0.006	0.016	0.007	0.027	0.001
C16	0.055	0.128	0.020	0.055	0.018	0.089	0.023	0.098	0.024	0.013	0.047	0.005
C17	0.040	0.064	0.004	0.008	0.000	0.000	0.000	0.000	0.000	0.003	0.015	0.002
C18	0.014	0.029	0.012	0.033	0.013	0.068	0.018	0.076	0.025	0.024	0.066	0.012
O19	0.058	0.016	0.087	0.032	0.084	0.027	0.055	0.028	0.095	0.057	0.052	0.037
N20 (R_i)			0.043	0.025	0.054	0.024	0.061	0.002				

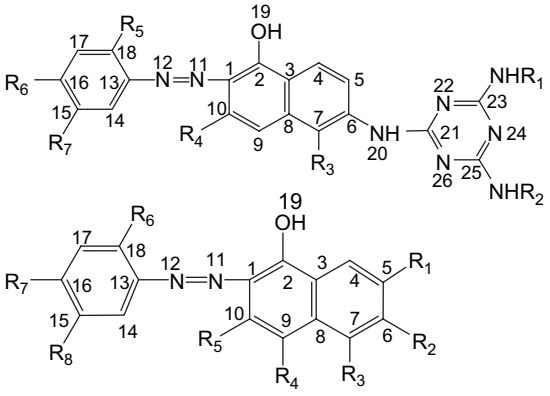

[a] Orange JVS (R_1 = *m*-sulfophenyl; R_2 = *m*-(2-hydroxyethylsulfonyl)phenyl; $R_3 = R_7 = H$; $R_4 = R_5 = SO_3H$; $R_6 = OCH_3$).
[b] Orange 7 ($R_1 = NHCOCH_3$; $R_2 = R_3 = R_4 = R_6 = R_7 = H$; $R_5 = SO_3H$; R_8 = VS).
[c] Orange 16 ($R_1(20) = NHCOCH_3$; $R_2 = R_3 = R_4 = R_6 = R_8 = H$; $R_5 = SO_3H$; R_7 = VS).
[d] Orange 72 ($R_2(20) = NHCOCH_3$; $R_1 = R_3 = R_4 = R_6 = R_8 = H$; $R_5 = SO_3H$; R_7 = VS).
[e] Red 22 ($R_1 = R_2 = R_4 = R_5 = R_7 = H$; $R_3 = SO_3H$; $R_6 = OCH_3$; R_8 = VS).
[f] Red NW ($R_1 = R_2 = R_3 = R_5 = H$; $R_4 = SO_3H$; $R_6 = OCH_3$; R_7 = VS; $R_8 = CH_3$).
VS = 2-hydroxyethylsulfonyl.

should be excluded. The low reactivity at N11═N12 may also be attributed to the very high energy barrier to the [2 + 2] addition, about 25 kcal mol^{-1} larger than that to the [2 + 2] addition at C13═C18 and C5═C10, as described in a previous paper [12]. The $S^{(E)}_{m,n}$ values corroborate this view, indicating that the values of the last two bonds are below the least two values of the potential positions.

The main reaction schemes for the ATs of Red gVS, ene (C1═C2; H(N20)) and [2 + 2] addition (C1═C2), are illustrated in Scheme 1(a) and (b). As Scheme 1 shows, these two modes of reaction may yield a common end product, *o*-(2-hydroxyethylsulfonyl)phenol (oVSPhe), bound to cellulose as the main decomposed product, although the decomposed products of the primary reaction of the first stage were different from each other. When the secondary main reaction modes, ene (C8═C9; H(O19)) and [2 + 2] addition (C8═C9), occurred, the rates of reaction were considerably lower than those for the main reactions at C1═C2; the secondary main reaction (a small number of rings opening at C8 and C9) may correspond to the slower decrease in the near-UV region at the early stage of fading (Fig. 1a). As will be seen below, the higher the rates of the main reactions, the clearer the absorption spectra of the decomposed products. Although the decomposed products of the third and subsequent reactions may be contained further, its confirmation became more difficult.

The absorption spectra of the decomposed products (Fig. 1a) were found to possess a high peak below 200 nm and two shoulders at 223 nm and 265 nm. The similarity of these spectra to those of Red 2RVS (which has the same diazo component) and Red pgVS suggests a resemblance in the reaction schemes (cf. Table 6).

3.5.1.2. ATs of Red mgVS. The order of reactivity based on the $\Delta_f H^0$(gas) values for the reaction products listed in Tables 7 and 8 was as follows:

ene (C8═C9; H(O19)) ≫ [2 + 2] addition (C3═C4)
≈ [2 + 2] addition (C8═C9) > ene(C1═C2; H(N20))
> [2 + 2] addition (C1═C2) > [2 + 2] addition
(C13═C18) ≈ [2 + 2] addition (C13═C14)

Table 6
Azo–hydrazone tautomerism, reaction modes of reaction with molecular singlet oxygen and its probable site for red reactive azo dyes from γ-, J- and 2R-acids

	Dyes	Tautomer (phase)	Ene (site)	[2 + 2] Addition (site)		
			In common	In common	Uniquely probable	Uniquely excluded
1	Red gVS	AT(g&w)	C1=C2, C8=C9	C1=C2, C5=C10, C6=C7, C8=C9	C13=C14, C13=C18	
2	Red pgVS					
3	Red mgVS					
4	Red gTri				C4=C5,C13=C14, C13=C18,C16=C17	
5	Red 2RVS				C13=C14, C13=C18	C5=C10
6	Orange 16[a]	HT(g&w)	C1=N11	C1=N11, C4=C5, C9=C10, C13=C14, C13=C18		
7	Orange 72[a]					
8	Orange JVS	AT(g) → HT(w) HT(g) → AT(w)		AT: C1=C2,C4=C5, C6=C7, C9=C10	C14=C15, 16=C17	
9	Red 22[a]					
10	Orange 7[a]	A/HT(g) → HT(w)	AT: C1=C2 HT: C1=N11	C13=C14, C13=C18. HT: C1=N11, C6=C7, C9=C10, C13=C14, C13=C18		AT: C9=C10
11	Red NW					

[a] C.I. reactive generic name.

$$> [2 + 2]\,\text{addition (C16=C17)} > [2 + 2]\,\text{addition (C5=C10)} > [2 + 2]\,\text{addition (C6=C7)} > [2 + 2]\,\text{addition (C15=C16)} \gg [2 + 2]\,\text{addition (N11=N12)}. \quad (4)$$

The orders of reactivity for Red gVS and Red mgVS based on the $S^{(E)}_{m,n}$ values were identical (cf. Table 2), but inequality (4) was different from inequality (3). The $S^{(E)}_{m,n}$ values for both dyes varied markedly at the corresponding sites of the two dyes. The contribution of the double bonds to the reactivity was also elucidated by plotting the $S^{(E)}_{m,n}$ values against $\log k_0$; the plot of $S^{(E)}_{m,n}(m, n: 1, 2; 5{-}10)$ against $\log k_0$ coincided well with the common correlation line. The contribution of the double bonds C13=C14, C13=C18 and C15=C16 was regarded as negligible, in addition to the double bonds C16=C17 and C3=C4 in the case of Red gVS. The double bonds are listed in the lower part of the corresponding column in Table 2. These double bonds contribute only slightly to the reactivity, due to the small values of $f^{(E)}_r$ and/or d_{HOMO} at C3, N11, C15, C16 and C18. Taken together with the molecular features of Red gVS, the $f^{(E)}_r$ values at C3, N11, C14, C16, and C18 show that these bonds are at the lower limit of contribution to the reactivity. The merely slight reactivity at the double bond N11=N12 may also be attributed to the very high energy barrier to the [2 + 2] addition, about 25 kcal mol^{-1} larger than that to the [2 + 2] addition at C15=C16.

The five dyes derived from γ- and 2R-acids may share similar mechanisms, as summarized in Tables 6 and 2. But the absorption spectra of the decomposed products on cellophane seem to have been determined by the diazo components. The spectra of Red mgVS were quite similar to those of Red 22, as shown in Fig. 2a and b. The main component may be *o*-methoxy-*m*-(2-hydroxyethylsulfonyl)phenol, and this could also be the main component of Red 22 as well. The slower decrease in the near-UV region at the early stage of fading may correspond to the ring opening at C8 and C9, the secondary main reaction. The spectra were the same as those for Yellow 17 and Pyr-Yellow [11]. These facts may support the reaction mechanism proposed. The resemblance in the spectra of the decomposed products demonstrates that the main reaction site is the double bond C1=C2, which means that the result is phenol formation and azo scission. The reaction schemes ene (C1=C2; H(N20)) and [2 + 2] addition (C1=C2) may both yield the same decomposed products bound to cellulose. Thus, the absorption spectra of the decomposed products may support the main reaction mechanism proposed.

3.5.1.3. ATs of Red pgVS. The order of reactivity based on the $\Delta_f H^0$(gas) values for the reaction products listed in Tables 7 and 8 was as follows:

$$\text{ene (C8=C9; H(O19))} \gg \text{ene(C1=C2; H(N20))} \approx [2 + 2]\,\text{addition (C8=C9)} > [2 + 2]\,\text{addition (C1=C2)} \approx [2 + 2]\,\text{addition (C3=C4)} \gg [2 + 2]\,\text{addition (C13=C14)} = [2 + 2]\,\text{addition (C13=C18)} > [2 + 2]\,\text{addition (C6=C7)} > [2 + 2]\,\text{addition (C16=C17)} = [2 + 2]\,\text{addition (C15=C16)} \approx [2 + 2]\,\text{addition (C5=C10)} \gg [2 + 2]\,\text{addition (N11=N12)}. \quad (5)$$

The orders of reactivity based on the $S^{(E)}_{m,n}$ values were identical for Red gVS, Red mgVS and this dye (cf. Table 2), but inequalities (3), (4) and (5) were markedly different from each other. Each dye had a distinct set of $S^{(E)}_{m,n}$ values, markedly different from those of the other dyes. The contribution of the double bonds to the reactivity was investigated by plotting the $S^{(E)}_{m,n}$ values against $\log k_0$. The double bonds of negligible contribution were identical to those in Red mgVS. The plot of $S^{(E)}_{m,n}(m, n: 1, 2; 5{-}10)$ against $\log k_0$ coincided well with the common correlation line.

As mentioned above (cf. Section 3.5.1.1), this dye derived from related diazo component may form *p*-(2-hydroxyethylsulfonyl)phenol as the photo-decomposed product; it closely

Table 7
Heat of formation, $\Delta_f H^0$(gas) (kcal mol^{-1}), of intermediate and products in the ene and [2 + 2] cycloaddition reactions at the double bonds of (C1═C2) and (C1═N11) for predominant tautomer of azo dyes derived from γ- and J-acids with singlet oxygen

	M.W.	$\Delta_f H^0$(gas) of intermediate at TSG	$\Delta_f H^0$(gas) of intermediate	$\Delta_f H^0$(gas) of hydroperoxide	$\Delta_f H^0$(gas) of intermediate at TSG	$\Delta_f H^0$(gas) of intermediate	$\Delta_f H^0$(gas) of addition product
Mode (site)		Ene (C1═C2;H(N20)) for AT			[2 + 2] Addition (C1═C2) for AT		
Red gVS	483.467	−152.107	−152.102	−169.319	−153.198	−153.186	−177.836
Red mgVS	513.493	−189.894	−189.849	−220.390	−187.836	−187.729	−217.310
Red pgVS	483.467	−154.027	−154.026	−188.122	−153.991	−153.891	−180.751
Red 2RVS	563.525	−268.205	−268.180	−311.253	−266.028	−266.012	−294.263
Red gTri	764.712	−250.921	−250.846	−282.572	−252.361	−252.165	−278.256
Mode (site)		Ene (C8═C9;H(O19)) for AT			[2 + 2] Addition (C8═C9) for AT		
Red gVS	483.467	−153.601	−153.593	−199.746	−152.270	−152.267	−184.694
Red mgVS	513.493	−190.173	−190.171	−236.993	−189.972	−189.972	−224.829
Red pgVS	483.467	−154.235	−154.215	−203.726	−155.035	−155.032	−187.684
Red 2RVS	563.525	−268.325	−268.275	−315.661	−268.383	−268.275	−302.448
Red gTri	764.712	−250.944	−250.726	−301.877	−251.940	−251.940	−281.571
Mode (site)		Ene (C1═C2;H(O19)) for AT			[2 + 2] Addition (C1═C2) for AT		
Orange JVS	934.895	−331.829	−331.821	−375.038	−331.802	−331.686	−362.127
Orange 7	525.504	−196.601	−196.601	−239.594	−195.766	−195.652	−229.733
Orange 16	525.504	−196.296	−196.290	−244.054	−196.367	−196.324	−229.070
Orange 72	525.504	−199.175	−199.166	−244.830	−196.771	−196.759	−228.271
Red 22	498.479	−187.055	−187.026	−233.079	−187.021	−187.019	−215.916
Red NW	512.505	−191.200	−191.172	−230.420	−191.277	−191.270	−213.557
Mode (site)		Ene (C1═N11;H(N12)) for HT			[2 + 2] Addition (C1═N11) for HT		
Orange JVS	934.895	−330.805	−330.802	−374.772	−330.976	−330.967	−338.642
Orange 7	525.504	−195.950	−195.912	−241.799	−195.995	−195.993	−200.262
Orange 16	525.504	−199.773	−199.758	−244.049	−199.746	−199.722	−207.074
Orange 72	525.504	−198.703	−198.703	−241.177	−198.690	−198.679	−206.698
Red 22	498.479	−189.692	−189.665	−230.294	−188.287	−188.280	−194.249
Red NW	512.505	−191.200	−191.192	−228.250	−191.277	−191.270	−194.251
	M.W.	$\Delta_f H^0$(gas) of intermediate at TSG	$\Delta_f H^0$(gas) of intermediate	$\Delta_f H^0$(gas) of addition product	$\Delta_f H^0$(gas) of intermediate at TSG	$\Delta_f H^0$(gas) of intermediate	$\Delta_f H^0$(gas) of addition product
Mode (site)		[2 + 2] Addition (C3═C8) for AT			[2 + 2] Addition (C3═C8) for HT		
Orange JVS	934.895	−331.984	−331.975	−336.400	−332.190	−332.190	−342.610
Orange 7	525.504	−195.947	−195.870	−200.485	−196.139	−196.138	−208.575
Orange 16	525.504	−196.417	−196.415	−201.294	−197.879	−197.834	−205.806
Orange 72	525.504	−197.052	−197.049	−201.768	−198.583	−198.483	−210.332
Red 22	498.479	−187.071	−187.069	−194.775	−188.012	−188.012	−200.921
Red NW	512.505	−191.293	−191.233	−199.837	−191.379	−191.376	−202.882
Mode (site)		[2 + 2] Addition (C4═C5) for AT			[2 + 2] Addition (C4═C5) for HT		
Orange JVS	934.895	−331.984	−331.975	−353.566	−332.131	−332.111	−346.059
Orange 7	525.504	−195.947	−195.870	−223.649	−196.009	−196.002	−218.159
Orange 16	525.504	−196.265	−196.264	−223.717	−197.446	−197.434	−219.641
Orange 72	525.504	−197.178	−197.173	−222.150	−198.245	−198.241	−218.816
Red 22	498.479	−187.091	−187.089	−209.300	−187.918	−187.850	−204.208
Red NW	512.505	−191.266	−191.201	−216.916	−191.312	−191.229	−216.919

resembles the *o*-isomer from the viewpoint of the absorption spectra and follows the same mechanism as the *o*-isomer. The similarity in the reaction scheme and the products to those of Red gVS are demonstrated by the similarity of the absorption spectra of the decomposed products.

3.5.1.4. ATs of Red 2RVS. This dye is 3-sulfo-substituted Red gVS. Despite being called 2R-acid and having an additional sulfonic acid group, it belongs to the arylazo-γ-acid group.

The order of reactivity based on the $\Delta_f H^0$(gas) values for the reaction products listed in Tables 7 and 8 was as follows:

$$\text{ene}\,(\text{C8═C9};\text{H(O19)}) > \text{ene}\,(\text{C1═C2};\text{H(N20)}) \approx [2+2]\ \text{addition}\,(\text{C8═C9}) \gg [2+2]\ \text{addition}\,(\text{C1═C2}) > [2+2]\ \text{addition}\,(\text{C3═C4}) > [2+2]\ \text{addition}\,(\text{C6═C7}) \approx [2+2]\ \text{addition}\,(\text{C16═C17}) \approx [2+2]\ \text{addition}\,(\text{C13═C14}) > [2+2]\ \text{addition}\,(\text{C15═C16}) = [2+2]\ \text{addition}\,(\text{C13═C18}) > [2+2]\ \text{addition}\,(\text{C5═C10}) \gg [2+2]\ \text{addition}\,(\text{N11═N12}). \quad (6)$$

The orders of reactivity for the double bonds in Red gVS, Red mgVS, Red pgVS, Red gTri (cf. Section 3.5.1.5) and

Table 8
Heat of formation, $\Delta_f H^0$(gas) (kcal mol^{-1}), of intermediate and products in the [2 + 2] cycloaddition reactions at the possible double bonds of dyes with singlet oxygen

	M.W.	$\Delta_f H^0$(gas) of intemediate at TSG	$\Delta_f H^0$(gas) of intermediate	$\Delta_f H^0$(gas) of hydroperoxide	$\Delta_f H^0$(gas) of intermediate at TSG	$\Delta_f H^0$(gas) of intermediate	$\Delta_f H^0$(gas) of addition product
Mode		[2 + 2] Addition (C6=C7) for AT			[2 + 2] Addition (C3=C4) for AT		
Red gVS	483.467	−152.174	−152.173	−164.144	−153.223	−153.171	−181.556
Red mgVS	513.493	−189.830	−189.782	−203.546	−187.836	−187.647	−225.094
Red pgVS	483.467	−155.168	−155.155	−167.666	−154.019	−153.882	−179.555
Red 2RVS	563.525	−269.394	−269.332	−289.095	−265.669	−265.509	−291.830
Red gTri	764.712	−253.999	−253.990	−262.876	−252.525	−252.525	−279.671
Mode		[2 + 2] Addition (C4=C5) for AT					
Red gVS	483.467	−150.988	−150.924	−152.631			
Red mgVS	513.493	−190.307	−190.294	−193.417			
Red pgVS	483.467	−153.854	−153.766	−155.954			
Red 2RVS	563.525	−269.713	−269.711	−280.097			
Red gTri	764.712	−252.222	−252.210	−247.525			
Mode		[2 + 2] Addition (C13=C14) for AT			[2 + 2] Addition (C13=C18) for AT		
Red gVS	483.467	−152.275	−152.274	−172.678	−152.394	−152.393	−161.602
Red mgVS	513.493	−190.042	−190.042	−210.473	−190.091	−190.078	−211.635
Red pgVS	483.467	−154.019	−153.998	−169.925	–	–	–
Red 2RVS	563.525	−268.319	−268.127	−288.283	−268.400	−268.291	−277.943
Red gTri	764.712	−252.057	−252.056	−271.294	−252.302	−252.284	−259.483
Mode		[2 + 2] Addition (C15=C16) for AT			[2 + 2] Addition (C16=C17) for AT		
Red gVS	483.467	−152.190	−152.133	−168.623	−152.284	−152.279	−173.502
Red mgVS	513.493	−190.085	−190.080	−196.583	−190.098	−190.089	−207.202
Red pgVS	483.467	−153.968	−153.963	−161.225	–	–	–
Red 2RVS	563.525	−268.267	−268.248	−284.959	−268.300	−268.225	−288.941
Red gTri	764.712	−252.015	−251.985	−268.347	−252.459	−252.440	−271.919
Mode		[2 + 2] Addition (N11=N12) for AT			[2 + 2] Addition (C5=C10) for AT		
Red gVS	483.467	−152.159	−152.144	−137.327	−153.191	−153.174	−161.622
Red mgVS	513.493	−190.741	−190.735	−174.790	−187.885	−187.803	−205.358
Red pgVS	483.467	−153.849	−153.845	−136.201	−154.035	−153.876	−160.614
Red 2RVS	563.525	−268.277	−268.261	−256.240	−265.724	−265.711	−275.037
Red gTri	764.712	−252.048	−252.025	−233.541	−252.324	−252.228	−258.982
Mode		[2 + 2] Addition (N11=N12) for AT					
Orange JVS	934.895	−330.842	−330.836	−312.278			
Orange 7	525.504	−198.007	−197.998	−179.192			
Orange 16	525.504	−196.321	−196.233	−177.192			
Orange 72	525.504	−197.635	−197.625	−178.990			
Red 22	498.479	−187.226	−187.116	−170.717			
Red NW	512.505	−191.280	−191.234	−173.001			

Red 2RVS, based on the $S^{(E)}_{m,n}$ values showing the first to third largest reactivity, were identical, although the $\Delta_f H^0$(gas) values were different. As with the three dyes mentioned above together with Red gTri, when the double bonds with larger $S^{(E)}_{m,n}$ values were picked from among the potential double bonds, a good common correlation was obtained by plotting $S^{(E)}_{m,n}$ against $\log k_0$ using all the double bonds mentioned in inequality (6). The plot of $S^{(E)}_{m,n}(m,n: 1,2;6-9,14,13,$ and $18)$ against $\log k_0$ showed a very good fit to the common line, as illustrated in Fig. 5. The merely slight contribution of the double bonds C16=C17, C3=C4, C5=C10 and N11=N12 to the reactivity may be attributed to the small values of d_{HOMO} and/or $f^{(E)}_r$ at the either end of the bonds, in spite of the considerable values of $f^{(E)}_r$ at the either end of the bonds. The low reactivity at the double bond N11=N12 may also be attributed to the very high energy barrier to the [2 + 2] addition, about 20 kcal mol^{-1} larger than that to the [2 + 2] addition at C5=C10, as described above and in a previous paper [11].

The absorption spectra of this dye's decomposed products agreed very well with those of Red gVS's decomposed products; the spectra are given in Fig. 1(a) and (b), respectively. The sulfonic acid group at position 3 in the naphthalene ring had little effect on the reaction mechanism (cf. Table 6) and only a small effect on the d_{HOMO}. Although whether or not this is a general property of the sulfonic acid groups in 2R-acid is not clear, Red 2RVS has smaller values of d_{HOMO} at C5 and C10 than the values for the azo dyes derived from γ-acid, as summarized in Table 5 and tabulated in Table 6, resulting in a higher stability of Red 2RVS against singlet oxygen than that of the dyes derived from γ-acid. The main reaction for Red 2RVS may be outlined by Scheme 1, if the corresponding substituents are inserted.

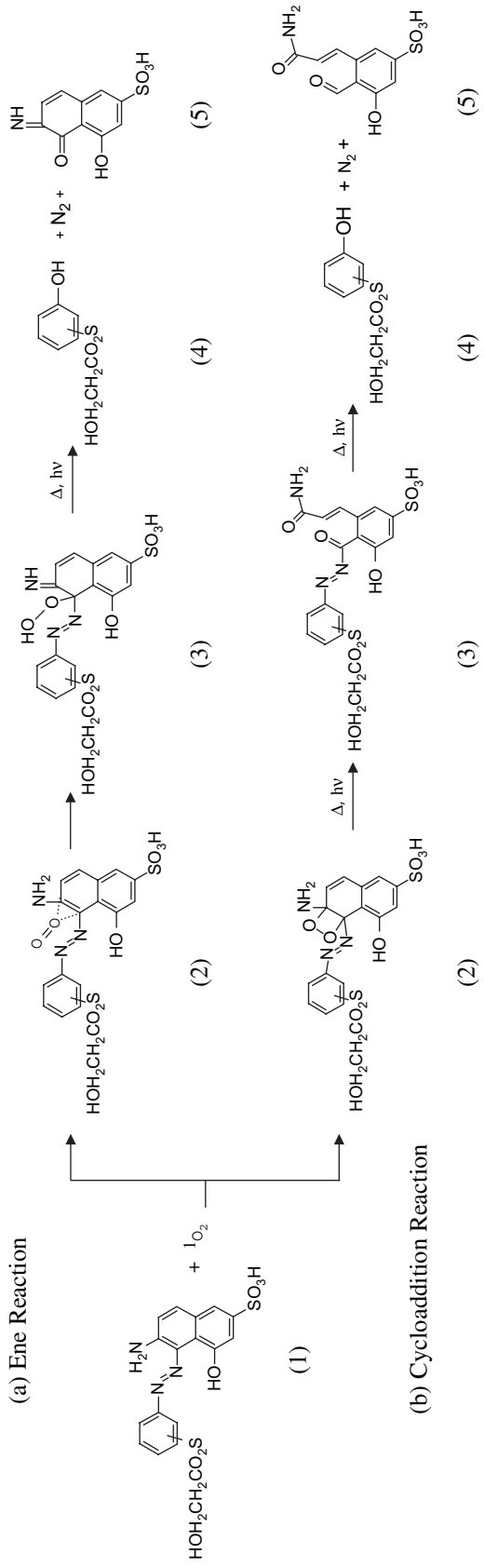

Scheme 1. (a) Ene (C1═C2; H(N20)) and (b) [2 + 2] cycloaddition (C1═C2) reactions of the ATs of a model azo dye from γ-acid (1), which contains a vinylsulfonyl anchor in the diazo component, with singlet oxygen. In (a), (2): ene intermediate by the addition of singlet oxygen to the double bond at C1═C2, (3): the hydroperoxide via ene reaction, (4) and (5): thermal and/or photo-decomposed products from the hydroperoxide via dediazotization, where some by-products other than (4) and (5) may be formed. In (b), (2): 1,2-dioxetane via [2 + 2] cycloaddition (the intermediate by the parallel addition of $^1O_2$ to the double bond of C1═C2 was omitted), (3) thermal and/or photo-decomposed products from the 1,2-dioxetanes, scission of C1═C2 bond, (4) and (5): thermal and/or photo-decomposed products from (3) via dediazotization, where some by-products other than (4) and (5) may be formed.

3.5.1.5. ATs of Red gTri. The order of reactivity based on the $\Delta_f H^0$(gas) values for the reaction products listed in Tables 7 and 8 was as follows:

$$\begin{aligned}&\text{ene (C8═C9; H(O19))} > \text{ene(C1═C2; H(N20))} > [2+2]\\&\text{addition (C8═C9)} > [2+2]\text{ addition (C3═C4)} > [2+2]\\&\text{addition (C1═C2)} > [2+2]\text{ addition (C16═C17)} \approx [2+2]\\&\text{addition (C13═C14)} > [2+2]\text{ addition (C15═C16)}\\&> [2+2]\text{ addition (C6═C7)} > [2+2]\text{ addition (C13═C18)}\\&\approx [2+2]\text{ addition (C5═C10)} \gg [2+2]\\&\text{addition (N11═N12).}\end{aligned} \tag{7}$$

Although the $S^{(E)}_{m,n}$ values varied with the dye, the five dyes resembled each other from the viewpoint of the order of reactivity based on the $S^{(E)}_{m,n}$ values. Among double bonds mentioned in inequality (7), the double bonds that contributed to the reactivity were determined by plotting the $S^{(E)}_{m,n}$ values against $\log k_0$. Thus, the plot of $S^{(E)}_{m,n}(m,n: 1,2,4{-}10,13,14,16{-}18)$ against $\log k_0$ fits the common correlation line very well.

This dye was confirmed to possess the largest reactivity among the phenylazo-γ-acid dyes in spite of having triazinyl groups; generally, dyes with this group have low reactivities, as demonstrated in a previous paper [12]. The triazine group of this particular dye seems to heighten the reactivities of all the possible double bonds (cf. Table 3). The contribution of the double bond N11═N12 may be excluded due to the very high energy barrier to the [2 + 2] addition, about 25 kcal mol^{-1} larger than that to the [2 + 2] addition at C5═C10.

The absorption spectra of the exposed sample in the visible region decreased with exposure time, while the absorption spectra in the UV region at wavelengths shorter than 350 nm did not decrease, indicating that the large triazinyl anchor group remained unchanged (Fig. 3a). The spectra in the UV region looked quite similar in shape to those of Yellow 2 [11], the anchor groups of these two dyes being geometrical isomers. Frontier orbital theory, in which the reactivity against $^1O_2$ at atomic position r is described as $f^{(E)}_r$, suggests that the potentially reactive positions are concentrated within the chromophore groups, and that triazinyl anchor groups do not contribute to the reactivity. The absorption spectra of the decomposed products should demonstrate this hypothesis unequivocally.

Red gTri and Yellow 2 [11], which possess very different diazo components and geometrically isomeric reactive anchors, yielded very similar decomposed products. This fact may also support the validity of the proposed reaction mechanism.

3.5.2. Reaction modes of Orange 7, Orange 16, Orange 72 and Red 22

Orange 7, Orange 16 and Orange 72 are geometrical isomers, with acetylamino and 2-hydroxyethylsulfonyl groups at different positions. The $\Delta_f H^0$(gas) and $\Delta_f H^0$(H_2O) values for their ATs and HTs indicate that the three orange dyes exist as HTs in both the gas phase and water, although Orange 7 also contains a small amount of ATs in the gas phase (cf.

Table 3). Thus, for Orange 7 only the reactivity of the ATs was analyzed. Like the three orange dyes, Red 22 exists as HTs in both the gas phase and water.

3.5.2.1. Reaction modes for the HTs of Orange 16. Based on the $\Delta_f H^0$(gas) values of each reaction product, listed in Tables 7–9, the following order of reactivity for the corresponding reaction modes was determined:

ene (C1═N11; H(N12)) ≫ [2 + 2] addition (C9═C10) > [2 + 2] addition (C13═C14) = [2 + 2] addition (C13═C18) > [2 + 2] addition (C4═C5) > [2 + 2] addition (C6═C7) > [2 + 2] addition (C17═C18) > [2 + 2] addition (C1═N11) > [2 + 2] addition

Table 9
Heat of formation, $\Delta_f H^0$(gas) (kcal mol^{-1}), of intermediates and products in the ene and [2 + 2] cycloaddition reactions at the possible double bonds for the predominant tautomer of dyes with $^1O_2$

	M.W.	$\Delta_f H^0$(gas) of intemediate at TSG	$\Delta_f H^0$(gas) of intermediate	$\Delta_f H^0$(gas) of hydroperoxide	$\Delta_f H^0$(gas) of intermediate at TSG	$\Delta_f H^0$(gas) of intermediate	$\Delta_f H^0$(gas) of addition product
Mode		[2 + 2] Addition (C6═C7) for AT			[2 + 2] Addition (C6═C7) for HT		
Orange JVS	934.895	−332.138	−332.130	−358.243	−332.349	−332.339	−350.755
Orange 7	525.504	−195.888	−195.695	−220.872	−196.079	−195.948	−215.386
Orange 16	525.504	−196.193	−196.159	−220.173	−197.479	−197.343	−216.204
Orange 72	525.504	−197.156	−197.014	−221.893	−199.232	−199.231	−219.099
Red 22	498.479	−187.166	−187.157	−204.063	−188.038	−187.995	−204.066
Red NW	512.505	−191.164	−191.160	−214.791	−191.334	−191.314	−210.947
Mode		[2 + 2] Addition (C9═C10) for AT			[2 + 2] Addition (C9═C10) for HT		
Orange JVS	934.895	−334.023	−334.021	−353.562	−334.145	−334.138	−359.585
Orange 7	525.504	−196.157	−196.147	−217.034	−196.294	−196.292	−222.749
Orange 16	525.504	−198.416	−198.408	−217.411	−197.567	−197.521	−224.719
Orange 72	525.504	−199.658	−199.651	−218.024	−201.464	−201.457	−225.266
Red 22	498.479	−187.107	−187.096	−215.939	−188.038	−187.995	−224.036
Red NW	512.505	−191.424	−191.195	−208.139	−191.499	−191.292	−217.485
Mode		[2 + 2] Addition (C13═C14) for AT			[2 + 2] Addition (C13═C14) for HT		
Orange JVS	934.895	−332.213	−332.143	−341.095	−333.189	−333.189	−343.433
Orange 7	525.504	−198.036	−198.034	−211.895	−198.135	−198.126	−217.104
Orange 16[a]	525.504	−196.198	−196.195	−216.755	−197.494	−197.390	−220.983
Orange 72	525.504	−197.538	−197.539	−212.679	−198.903	−198.760	−216.633
Red 22	498.479	−187.151	−187.133	−207.077	−187.936	−187.933	−207.947
Red NW	512.505	−191.256	−191.215	−209.030	−191.274	−191.249	−209.036
Mode		[2 + 2] Addition (C13═C18) for AT			[2 + 2] Addition (C13═C18) for HT		
Orange JVS	934.895	−334.199	−334.192	−350.646	−332.057	−331.994	−353.217
Orange 7	525.504	−196.128	−196.113	−211.684	−196.402	−196.367	−216.738
Red 22	498.479	−187.062	−187.058	−208.482	−187.977	−187.942	−210.170
Red NW	512.505	−191.316	−191.298	−212.109	−191.390	−191.378	−212.559
Mode		[2 + 2] Addition (C15═C16) for AT			[2 + 2] Addition (C15═C16) for HT		
Orange JVS	934.895	−330.202	−330.163	−356.043	−333.034	−332.999	−357.315
Orange 7	525.504	−196.048	−196.041	−204.802	−196.212	−196.212	−204.144
Orange 16[a]	525.504	−198.289	−198.268	−205.055	−197.515	−197.504	−205.591
Orange 72[a]	525.504	−196.891	−196.871	−212.643	−197.075	−196.987	−213.852
Red 22	498.479	−186.899	−186.861	−192.508	−188.016	−187.963	−193.935
Red NW	512.505	−191.239	−191.206	−200.733	−191.091	−191.062	−199.256
Mode		[2 + 2] Addition (C16═C17) for AT			[2 + 2] Addition (C16═C17) for HT		
Orange JVS	934.895	−332.140	−332.085	−354.577	−330.489	−330.480	−355.589
Orange 7	525.504	−195.975	−195.966	−211.678	−196.151	−195.999	−212.973
Red 22	498.479	−187.062	−187.058	−205.917	−187.930	−187.930	−207.351
Red NW	512.505	−191.165	−191.143	−217.852	−191.161	−191.074	−217.503
Mode		[2 + 2] Addition (C17═C18) for AT			[2 + 2] Addition (C17═C18) for HT		
Orange JVS	934.895	−332.147	−332.135	−343.075	−331.391	−331.360	−343.242
Orange 7	525.504	−196.596	−196.563	−212.034	−196.154	−196.103	−213.516
Orange 16	525.504	−196.244	−196.244	−213.660	−197.764	−197.716	−215.135
Orange 72	525.504	−190.686	−190.679	−215.806	−199.393	−199.389	−217.955
Red 22	498.479	−187.076	−186.888	−208.090	−188.012	−187.831	−210.142
Red NW	512.505	−191.321	−191.210	−217.913	−191.286	−191.266	−217.528

[a] Orange 16 and 72: The corresponding $\Delta_f H^0$(gas) values for [2 + 2] addition (C13═18) and (C16═17) were equal to those for [2 + 2] addition (C13═14) and (C15═16), respectively.

$$(\mathrm{C3{=}C8}) \approx [2+2]\ \text{addition}\ (\mathrm{C15{=}C16}) = [2+2]\ \text{addition}\ (\mathrm{C16{=}C17}). \quad (8)$$

The order of reactivity based on the $S^{(\mathrm{E})}_{m,n}$ values at each double bond mentioned in inequality (8), listed in Table 3, was considerably different from inequality (8). As the results of the azo dyes derived from γ-acid mentioned above and in the previous paper showed, however, good linear correlations were found between $S^{(\mathrm{E})}_{m,n}(m,n:)$ and $\log k_0$ for a series of azo dyes. Therefore, whether or not the potential double bonds of the dyes examined contribute to the reactivity of the dyes was determined based on this relationship. Since Orange 16 and Orange 72 exist as HTs and the five dyes mentioned above exist as ATs, the plots of $S^{(\mathrm{E})}_{m,n}(m,n:)$ may clarify the relationship more unequivocally than the $S^{(\mathrm{E})}_{m,n}(m,n:)$ plots for dyes whose AHT changes during the transition from the gas phase to water.

The plot of $S^{(\mathrm{E})}_{m,n}(m,n:1,11;4,5,9,10,14,13,\text{ and }18)$ against $\log k_0$ coincided well with the common correlation line. The merely slight contribution of the double bonds C3═C8, C6═C7 and C15═C16 to the reactivity may be attributed to the small values of d_{HOMO} and/or $f_{\mathrm{r}}^{(\mathrm{E})}$ at either end of the bonds, in spite of the considerable values of $f_{\mathrm{r}}^{(\mathrm{E})}$ at the either end of the bonds. The addition of the contribution from these double bonds, listed in Table 3, generated a corresponding deviation in the direction of higher reactivity, when they were plotted together with all the other dyes. The fact that this dye exists as HTs in both the gas phase and water and that the plot of the $S^{(\mathrm{E})}_{m,n}$ values for the HTs fits the common correlation line but not that for the ATs may indicate the validity of the present analysis based on MO theory.

As mentioned above (cf. Section 3.2), the decomposed products on cellulose of Orange 16, Orange 72 and Red pgVS, synthesized from the same diazo component, and of Orange 7, synthesized from the isomeric diazo component, should give the same absorption spectra only if the same main reaction scheme is valid for all of the four dyes. The spectra of the exposed samples and the decomposed products are given in Fig. 4 (Orange 7 (a), Orange 16 (b), Orange 72 (c) and Red pgVS (d)). The spectra showed an overall similar pattern, with a characteristic peak at 223 nm and a shoulder at 265 nm; however, they did not resemble each other in detail. The decomposed products of Red pgVS, the dye with the highest fading rate, showed the clearest double-shoulder spectral pattern. As expected, the dyes with lower fading rates had similar spectra, but the details of the patterns were vague.

As Scheme 2 shows, this dye may undergo ene (C1═N11; H(N12)) and [2 + 2] addition (C9═C10), which may generate *p*-(2-hydroxyethylsulfonyl)phenol as the end product via dediazotization, in spite of the addition to different double bonds. Orange 16 may also undergo [2 + 2] addition at other double bonds. The contribution of these bonds to the reactivity may be obscured due to that fact that the decomposed products may be mixed, generating unclear spectral patterns.

The results of a GC/MS analysis of the photo-oxidative degradation of Orange 16 in an aqueous solution by UV irradiation have been reported recently [35]. Some comments can

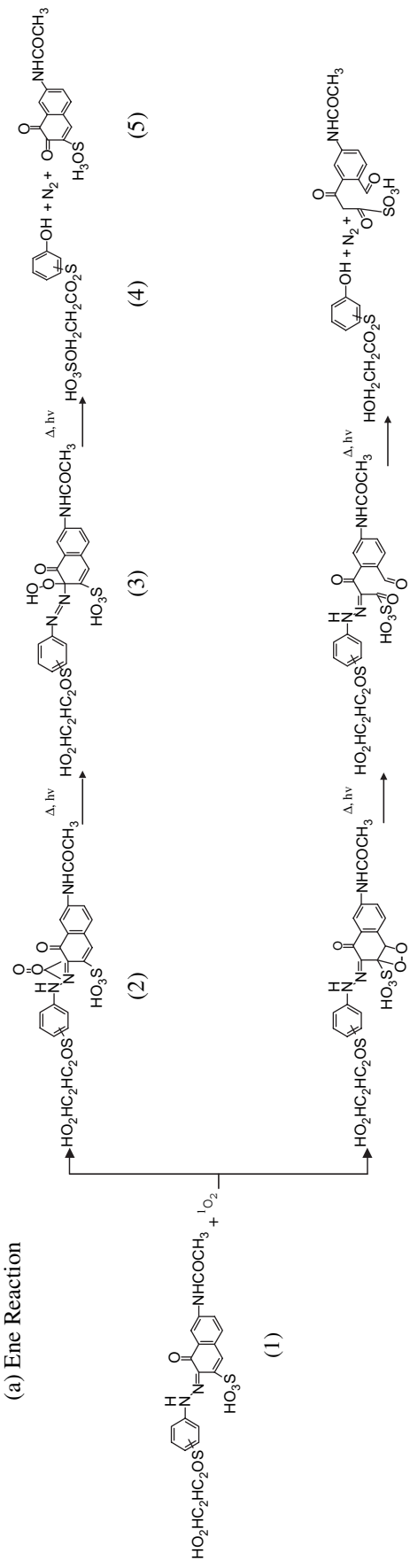

Scheme 2. (a) Ene (C1═N11; H(N12)) and (b) [2 + 2] cycloaddition (C9═C10) reactions of the HTs of a model benzene-azo-naphthalen dye (1), which contains a vinylsulfonyl anchor in the coupling component, with singlet oxygen. In (a), (2): ene intermediate by the addition of singlet oxygen to the double bond at C1═N11, (3): the hydroperoxide via ene reaction, (4) and (5): thermal and/or photo-decomposed products from the hydroperoxide via dediazotization, where some by-products other than (4) and (5) may be formed. In (b), (2): 1,2-dioxetane via [2 + 2] cycloaddition (C9═C10) (the intermediate by the parallel addition of $^1O_2$ to the double bond of C9═C10 was omitted), (3) thermal and/or photo-decomposed products from the 1,2-dioxetanes, scission of C9═C10 bond, (4) and (5): thermal and/or photo-decomposed products from (3) via dediazotization, where some by-products other than (4) and (5) may be formed. (See text.)

be made on that analysis from the viewpoint of the present study, as follows. The reaction intermediates of the first stage (probably the formation of the corresponding intermediates, shown in structure (2) of Scheme 1, via ene and/or [2 + 2] addition) may be decomposed further to yield the final decomposed products. The process of amine formation, which was assumed to be a result of photo-oxidation, may show simultaneous occurrence of photo-reduction. The results of the study in question may be consistent with those of our study, implying that it is difficult to elucidate the reaction mechanism simply by analyzing the decomposed products.

3.5.2.2. Reaction modes of the HTs for Orange 72. Based on the $\Delta_f H^0$(gas) values for each reaction product, the following order of reactivity for the corresponding reaction modes was established:

$$\begin{aligned}&\text{ene (C1=N11; H(N12))} > [2+2]\text{ addition (C9=C10)}\\ &> [2+2]\text{ addition (C13=C14)} > [2+2]\text{ addition}\\ &\text{(C6=C7)} > [2+2]\text{ addition (C13=C18)} > [2+2]\\ &\text{addition (C16=C17)} > [2+2]\text{ addition (C17=C18)}\\ &> [2+2]\text{ addition (C4=C5)} > [2+2]\text{ addition}\\ &\text{(C1=N11)} > [2+2]\text{ addition (C15=C16)}\\ &= [2+2]\text{ addition (C3=C8).}\end{aligned} \tag{9}$$

As with Orange 16, the potential double bonds for this dye are listed in Table 3. Although the corresponding atomic sites of Orange 16 and Orange 72 had different $f_r^{(E)}$ values, the pattern of reactivity and non-reactivity at the double bonds was the same for both dyes. Thus, the difference in the position of the acetylamino groups in the coupling component had little influence on the reactivity. The acetylamino groups had reverse or counterbalancing effects on the double bonds of C1=N11 and C4=C5 in Orange 16 and Orange 72, respectively. The plot of $S_{m,n}^{(E)}(m,n: 1,11,4,5,9,10,14,13,$ and $18)$ against $\log k_0$ coincided very well with the common correlation line. As with Orange 16, the addition of the contribution from the other double bonds led to a corresponding deviation in the direction of higher reactivity when Orange 72 was plotted together with all the other dyes. The five dyes, which existed as ATs, and the two dyes, which existed as HTs, determined the common correlation line between the $S_{m,n}^{(E)}$ values and $\log k_0$.

The absorption spectra of the decomposed products are illustrated in Fig. 4c. The same explanation as that given for Orange 16 may be applied to this dye as well. As shown in Scheme 2 (the position of the substituents should be modified accordingly), the HTs of this dye may undergo ene (C1=N11; H(N12)) and [2 + 2] addition (C1=N11), yielding *p*-(2-hydroxyethylsulfonyl)phenol as the main product. Besides these modes, [2 + 2] addition (C13=C14, C13=C18) may occur and may generate related biscarbonyl derivatives, which may result in a mixture of decomposed products.

3.5.2.3. Reaction modes of Orange 7. As mentioned above, Table 3 may indicate that Orange 7 exists overwhelmingly as HTs in water and the gas phase. A small number of Orange 7 ATs may exist in the gas phase as the minor component. Since we had no procedure for estimating the population ratio of tautomers in water-swollen cellulose, we focused mainly on the reaction modes of HTs, briefly analyzing those of ATs.

3.5.2.3.1. HTs. The $\Delta_f H^0$(gas) values for the reaction products at each double bond (cf. Tables 7–9) indicated the following order of reactivity for the corresponding reaction modes:

$$\begin{aligned}&\text{ene (C1=N11; H(N12))} > [2+2]\text{ addition}\\ &\text{(C9=C10)} > [2+2]\text{ addition (C4=C5)} > [2+2]\\ &\text{addition (C13=C14)} \approx [2+2]\text{ addition (C6=C7)}\\ &> [2+2]\text{ addition (C13=C18)} = [2+2]\\ &\text{addition (C17=C18)} \approx [2+2]\text{ addition (C16=C17)}\\ &> [2+2]\text{ addition (C3=C8)} > [2+2]\text{ addition}\\ &\text{(C15=C16)} > [2+2]\text{ addition (C1=N11).}\end{aligned} \tag{10}$$

The order of reactivity based on the $S_{m,n}^{(E)}$ values, listed in Table 3, was different from inequality (10). Among the double bonds mentioned above, the reactivities of the double bonds C3=C8, C15=C16 and C6=C7 may be excluded due to the small values of d_{HOMO} at C3 (0.003), C15 (0.003) and C6 (0.002). The reactivity at C17 may also be excluded due to the $f_r^{(E)}$ value, which is smaller than or similar to the values at C15 and C6. The plot of $S_{m,n}^{(E)}(m,n: 1,11;4,5,9,10,14,13,$ and $18)$ against $\log k_0$ showed a good coincidence with the common correlation line for a series of dyes. As mentioned above, even when this dye undergoes the transition from water, in which HTs predominate, to the gas phase, the AHT changes into a mixture of ATs and HTs, though HTs still constitute the main component. Therefore, it is reasonable to suppose that most of the dye molecules are HTs. The coincidence of the $S_{m,n}^{(E)}$ plot for the HTs with the common correlation line may also support this assumption. The fact that the ATs contribute little to the reactivity seems to show that the cellulose phase may be closer to the water phase than to the gas phase.

Orange 7 and Orange 16 are isomers, with the VS groups at different positions. Their patterns of reactivity and non-reactivity at the individual double bonds were identical. However, the reactivities or the sum of $f_r^{(E)}$ at five double bonds of Orange 7 were always larger than those at the corresponding sites of Orange 16. The VS groups, which were located at different positions, had higher influences on the activation of the double bonds C1=N11, C9=C10 and C4=C5 in the coupling component than the azo groups.

3.5.2.3.2. ATs. Although the ATs of this dye were found to exist as the minor component in the gas phase, their reaction mode was also analyzed. Based on the $\Delta_f H^0$(gas) values for the reaction products at each double bond with potential

reactivity (cf. Tables 7–9), the following order of reactivity for the corresponding reaction modes was determined:

ene (C1═C2; H(O19)) > [2 + 2] addition (C1═C2) > [2 + 2] addition (C4═C5) > [2 + 2] addition (C9═C10) > [2 + 2] addition (C6═C7) > [2 + 2] addition (C13═C14) ≈ [2 + 2] addition (C13═C18) ≈ [2 + 2] addition (C17═C18) > [2 + 2] addition (C15═C16) > [2 + 2] addition (C16═C17) > [2 + 2] addition (C3═C8) ≫ [2 + 2] addition (N11═N12). (11)

This order was different from the order based on the $S^{(E)}_{m,n}$ values, listed in Table 3. As in the cases already mentioned, it was necessary to determine whether or not the reactivity of the double bonds C3═C8, C15═C16, C13═C18, C17═C18 and N11═N12 may be excluded due to the small values of d_{HOMO} at C3 (0.001), C15 (0.003), C17 (0.004), N11 (0.006) and C18 (0.012). After eliminating the contribution from all these sites, the $S^{(E)}_{m,n}(m,n)$ values for the ATs were determined. It was found that the plot of $S^{(E)}_{m,n}(m,n: 1,2,4{-}7;9,10,14,13,18)$ against $\log k_0$ deviated markedly from the common correlation line in the direction of higher reactivity. The complete lack of contribution of the ATs to the reactivity of this dye on water-swollen cellulose may thus be indirectly demonstrated.

The absorption spectra of the decomposed products are shown in Fig. 4a. The characteristic shoulders at 223 nm may resemble those of Orange 16, which has a different isomeric diazo component. Compared with the spectra of Red pgVS, which have two clear shoulders, the spectral pattern of Orange 7 seems to be closer to that of Orange 16. The absorption spectra provided no clue to the contribution or lack thereof of the ATs to the reactivity.

As shown in Scheme 2 (the position of the substituents should be modified accordingly), the HTs of this dye may undergo ene (C1═N11; H(N12)), [2 + 2] addition (C1═N11, C9═C10), yielding *m*-(2-hydroxyethylsulfonyl)phenol as the main product. Besides these modes, [2 + 2] addition (C13═C14, C13═C18) may occur, generating related biscarbonyl derivatives, which may result in a mixture of decomposed products.

3.5.2.4. Reaction modes of the HTs for Red 22. Based on the $\Delta_f H^0$(gas) values for each reaction product, the following order of reactivity for the corresponding reaction modes was determined:

ene (C1═N11; H(N12)) > [2 + 2] addition (C9═C10) > [2 + 2] addition (C13═C18) ≈ [2 + 2] addition (C17═C18) > [2 + 2] addition (C13═C14) ≈ [2 + 2] addition (C16═C17) > [2 + 2] addition (C4═C5) ≈ [2 + 2] addition (C6═C7) > [2 + 2] addition (C3═C8) > [2 + 2] addition (C1═N11) ≈ [2 + 2] addition (C15═C16). (12)

The order of reactivity based on the $S^{(E)}_{m,n}$ values, listed in Table 3, is different from inequality (12). Among the double bonds mentioned above, the reactivities of the double bonds C4═C5 and C6═C7 may be excluded due to the small values of d_{HOMO} at C4 (0.006) and C6 (0.004). The plot of $S^{(E)}_{m,n}(m,n: 1,11;3,8.9,10,14,13,18,15,$ and $16)$ against $\log k_0$ coincided well with the common correlation line.

Among the four dyes of this group, Red 22 had the highest reactivity. This may be attributed to two positions, C1 and C9, which had highly concentrated values of $f^{(E)}_r$. The sum of the $f^{(E)}_r$ values for the double bonds of Red 22 was largest at C1═N11, C9═C10 and C3═C8.

The absorption spectra of the decomposed products for the HTs of Red 22 (Fig. 2b) showed a typical pattern, identical with that of the ATs of Red mgVS (Fig. 2a), the HTs of C.I. Reactive Yellow 17 [11] and the ATs of Pyr-Yellow [11], which possess the same diazo component bound with a VS anchor system. Considering the $f^{(E)}_r$ values for the double bonds C1═N11 and C9═C10, ene (C1═N11; H(N12)) and [2 + 2] addition (C1═N11, C9═C10) (the former two modes are illustrated in Scheme 2) may be the main reaction scheme, resulting in the same end product, 2-methoxy-5-(2-hydroxyethylsulfonyl)phenol via dediazotization. Scheme 3 illustrates the [2 + 2] addition reaction at C9═C10, which yields 2-methoxy-5-(2-hydroxyethylsulfonyl)phenol as the common end product mentioned above.

These results may demonstrate the validity of using the electrophilic frontier density to pinpoint the reaction of azo dyes against singlet oxygen.

3.5.3. Reaction modes of Orange JVS

The $\Delta_f H^0$(gas) and $\Delta_f H^0$ (H_2O) values indicated that this dye exists as ATs in the gas phase and as HTs in water. Although the tautomer of this dye on cellulose could not be determined, the reactivities of both tautomers in the gas phase were analyzed in terms of MO theory.

3.5.3.1. ATs. As in the previous studies, the double bonds with higher reactivities against $^1O_2$ were determined based on the electron density in the HOMO, listed in Table 5. The double bonds with possible reactivity are C1═C2, C4═C5, C6═C7, C13═C14, C13═C18, C15═C16, C17═C18, N11═N12 and C3═C8; this means that almost all of the double bonds possess potential reactivity. As in the previous studies [11,12], the $\Delta_f H^0$(gas) values for the reaction intermediates and products of each mode were calculated using the PM5 method (cf. Tables 7–9). The $\Delta_f H^0$(gas) values for the reaction intermediates were almost identical, as in the previous studies [11,12], and therefore no comparison between the modes was possible. The order of reactivity based on the $\Delta_f H^0$(gas) values for the reaction products was as follows:

ene (C1═C2; H(O19)) > [2 + 2] addition (C1═C2) > [2 + 2] addition (C6═C7) > [2 + 2] addition (C15═C16) ≈ [2 + 2] addition (C9═C10) > [2 + 2]

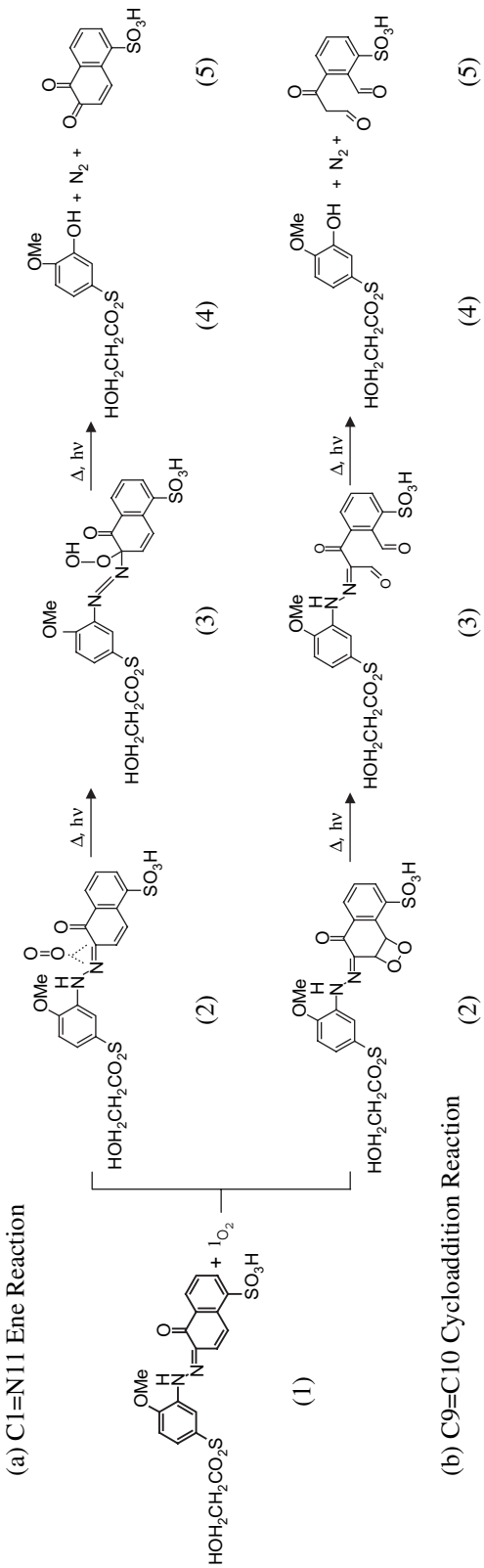

Scheme 3. (a) Ene (C1=N11; H(N12)) and (b) [2 + 2] cycloaddition (C9=C10) reactions of the HTs of Red 22 dye (1), which contains a vinylsulfonyl anchor in the diazo component, with singlet oxygen. In (a), (2): ene intermediate by the addition of singlet oxygen to the double bond at C1=N11, (3): the hydroperoxide via ene reaction, (4) and (5): thermal and/or photo-decomposed products from the hydroperoxide via dediazotization, where some by-products other than (4) and (5) may be formed. In (b), (2): 1,2-dioxetane via [2 + 2] cycloaddition (the intermediate by the parallel addition of $^1O_2$ to the double bond of C9=C10 was omitted), (3) thermal and/or photo-decomposed products from the 1,2-dioxetanes, scission of C9=C10 bond, (4) and (5): thermal and/or photo-decomposed products from (3) via dediazotization, where some by-products other than (4) and (5) may be formed. (See text.)

addition (C16=C17) > [2 + 2] addition (C4=C5) > [2 + 2] addition (C13=C18) > [2 + 2] addition (C17=C18) > [2 + 2] addition (C13=C14) > [2 + 2] addition (C3=C8) > [2 + 2] addition (N11=N12). (13)

Although we could not discriminate between ene and [2 + 2] addition based on the $S^{(E)}_{m,n}$ values, inequality (13) and the order of reactivity based on the $S^{(E)}_{m,n}$ values coincided, which may indicate that the reactivity of the ene reaction was higher than that of the [2 + 2] addition at C1=C2. In Tables 7–9, the $\Delta_f H^0$(gas) values for the HTs of the reaction intermediates and the products of each mode are also listed. Some of these values were smaller than those for the ATs, while others were the reverse. This may indicate that Orange JVS undergoes AHT during the reaction.

Among the double bonds mentioned above, C3=C8 may be excluded due to the very small value of d_{HOMO} at C3 (0.005) and C8 (0.003). Although the $f_r^{(E)}$ values at C5, C15, C18 and N11 are small, those of d_{HOMO} at the corresponding positions may exceed the lower limit. Therefore, the contributions of all double bonds listed in Table 3 for the ATs, except C3=C8, should be taken into consideration.

Plotting $S^{(E)}_{m,n}(m,n: 1,2;4–7;9–18)$ against $\log k_0$ may determine a point for the ATs of this dye in the figure of relationship between them. As mentioned below, after the plots of the other dyes were added, the plot of this dye showed a considerable deviation from the common correlation line in the direction of higher reactivity, as shown in Fig. 5.

3.5.3.2. HTs. The structural difference between ATs and HTs is that ATs have C1=C2, while HTs have C1=N11. The other double bonds are identical, although the $\Delta_f H^0$(gas) values for the corresponding reaction products may differ. Based on the $\Delta_f H^0$(gas) values for each reaction product, the following order of reactivity for the corresponding reaction modes was determined:

ene (C1=N11; H(N12)) > [2 + 2] addition (C15=C16) > [2 + 2] addition (C16=C17) > [2 + 2] addition (C9=C10) > [2 + 2] addition (C13=C18) > [2 + 2] addition (C6=C7) > [2 + 2] addition (C4=C5) > [2 + 2] addition (C1=N11) > [2 + 2] addition (C13=C14) ≈ [2 + 2] addition (C17=C18) > [2 + 2] addition (C3=C8). (14)

This order was partially different from that based on the $S^{(E)}_{m,n}$ values (cf. Table 3), indicating the existence of geometrical variations due to the interaction with $^1O_2$. As with the ATs, C3=C8 and C6=C7 may also be excluded due to the very small values of d_{HOMO} at C3 (0.002) and C6 (0.000). Although the $f_r^{(E)}$ values at C4 and C15 are small, those of d_{HOMO} at the corresponding positions may exceed the lower limit. Therefore, the contribution of all double bonds listed in Table 3 for the HTs should be taken into consideration, except for C3=C8 and C6=C7.

The plot of $S^{(E)}_{m,n}(m,n:1,4,5,9{-}11;13,14,16{-}18)$ against $\log k_0$ showed a large deviation from the common correlation line in the direction of smaller reactivity, despite the fact that almost all double bonds were taken into account. If the contributions to the reactivity of both the ATs and the HTs are taken into consideration, the reactivities estimated in terms of frontier orbital theory using the PM5 method might describe the reaction of this dye with $^1O_2$ well. Since the population ratio of the tautomers could not be estimated on water-swollen cellulose, we had no procedure by which to advance further in this analysis quantitatively.

The absorption spectra of the decomposed products bound to cellulose are shown in Fig. 3b. The decrease or fading of the visible absorption spectra with exposure time was observed, while no decrease of the spectra in the UV region under 350 nm occurred as with Red gTri (cf. Section 3.5.1.5), indicating that no degradation of the large triazinyl anchor groups occurred. The large absorption band under 350 nm may correspond to the 2,4-bis(substituted phenylamino)triazinyl anchor group.

According to frontier orbital theory, the anchor groups may contain no double bonds with which $^1O_2$ can react. $^1O_2$ may attack the double bonds in the chromophore part instead. The double bonds of Orange JVS with larger $f^{(E)}_r$ values are listed in Table 3 for both tautomers. The most highly reactive double bond may be C1=C2 for the ATs, and it can undergo ene (C1=C2; H(O19) or [2 + 2] addition (C1=C2). Scheme 1 may outline both modes, although the chemical structure should be modified accordingly. Dediazotization after the ene and/or [2 + 2] addition reaction splits off the azo groups, resulting in phenols connected with the anchor groups as the main decomposed products [11,12]. However, some aromatics other than phenols may be generated as well. The reaction scheme for the HTs may be inferred from Scheme 2, in analogy to Scheme 1 for the ATs.

As mentioned above, this dye may exist as a mixture of ATs (with high reactivity) and HTs (with low reactivity) on cellulose at a constant population ratio. Keeping this population ratio constant, the reaction with $^1O_2$ may progress.

3.5.4. Reaction modes of Red NW

The $\Delta_f H^0$(gas) and $\Delta_f H^0$ (H_2O) values indicated that Red NW exists as ATs in the gas phase and as HTs in water. This dye may tend to exist as HTs on cellulose. The reactivities of both tautomers and the AHT of the dye were analyzed.

3.5.4.1. ATs. Based on the $\Delta_f H^0$(gas) values for each reaction product, the following order of reactivity for the corresponding reaction modes was determined:

$$\begin{aligned}&\text{ene (C1=C2; H(O19))} > [2+2]\text{ addition (C16=C17)}\\ &= [2+2]\text{ addition (C17=C18)} > [2+2]\text{ addition}\\ &\text{(C4=C5)} > [2+2]\text{ addition (C6=C7)} > [2+2]\\ &\text{addition (C1=C2)} > [2+2]\text{ addition (C13=C18)}\\ &> [2+2]\text{ addition (C13=C14)} > [2+2]\text{ addition}\\ &\text{(C9=C10)} > [2+2]\text{ addition (C15=C16)} > [2+2]\\ &\text{addition (C3=C8)} > [2+2]\text{ addition (N11=N12).}\end{aligned} \tag{15}$$

The order of reactivity based on the $S^{(E)}_{m,n}$ values was different from inequality (15). Among the double bonds mentioned, the reactivity of the double bonds C3=C8, C9=C10 and C13=C14 may be excluded due to the small values of d_{HOMO} at C3 (0.000), C8 (0.001) C10 (0.002) and C14 (0.003). Since C13=C18 may have contributed to the reactivity, only C14 was excluded. As mentioned above, the double bond N11=N12 was excluded due to the very high energy barrier to the reaction. And so, the plot of $S^{(E)}_{m,n}(m,n:1,2;4{-}7;13,15{-}18)$ against $\log k_0$ showed a large deviation from the common correlation line for a series of dyes in the direction of higher reactivity.

3.5.4.2. HTs. Based on the $\Delta_f H^0$(gas) values for each reaction product, the following order of reactivity for the corresponding reaction modes was determined:

$$\begin{aligned}&\text{ene (C1=N11; H(N12))} > [2+2]\text{ addition (C9=C10)}\\ &= [2+2]\text{ addition (C16=C17)} = [2+2]\text{ addition}\\ &\text{(C17=C18)} > [2+2]\text{ addition (C4=C5)} > [2+2]\\ &\text{addition (C13=C18)} > [2+2]\text{ addition (C6=C7)}\\ &> [2+2]\text{ addition (C13=C14)} > [2+2]\text{ addition}\\ &\text{(C3=C8)} > [2+2]\text{ addition (C15=C16)}\\ &> [2+2]\text{ addition (C1=N11).}\end{aligned} \tag{16}$$

The order of reactivity based on the $S^{(E)}_{m,n}$ values was different from inequality (16). Due to the small values of d_{HOMO} at C6 (0.000), C17 (0.001), and C15 (0.004), it was necessary to determine first whether or not the double bonds C3=C8, C13=C16, C16=C17, C6=C7 and N11=C1 contributed to the reactivity of the dye. The plot of $S^{(E)}_{m,n}(m,n:1,2;4{-}7;13,15{-}18)$ against $\log k_0$ showed a large deviation from the common correlation line for a series of dyes in the direction of higher reactivity. The plot of $S^{(E)}_{m,n}(m,n:1,11;4,5,14,13,\text{ and }18)$ against $\log k_0$, however, coincided well with the common correlation line.

The absorption spectra of the decomposed products on cellulose for this dye showed an absorption peak at around 200 nm, and the UV bands were characteristic (Fig. 1c). The UV absorption for this dye was similar to that for C.I. Reactive Yellow 17 [11] at wavelengths under 300 nm. The UV spectra for the main component of the decomposed product may indicate 2-methoxy -5-methyl-4-(2-hydroxyethylsulfonyl)phenol.

The $f^{(E)}_r$ values listed in Table 2 show that the most reactive double bonds against $^1O_2$ may be C1=C2 and C4=C5 for the ATs and C4=C5, C8=C9, and C1=N11 for the HTs. The three double bonds C8=C9 and C1=N11 and C4=C5 may follow the same reaction scheme as that of Red 22 (cf. 3.5.2.4), yielding this main end product. Thus, frontier orbital

theory seems to be consistent with the reaction schemes proposed and with the absorption spectra observed for the decomposed products.

4. Summary

The photo-sensitized fading of 11 reactive azo dyes derived from γ-acid, J-acid and related naphthalene sulfonic acids on cellulose was examined by exposing the dyed films immersed in aerobic aqueous Rose Bengal solution to a carbon arc. From the initial rates of fading, the second-order rate constants (k_0) of reaction of the dyes and $^1O_2$ were determined using the k_0 value for Pyr-Yellow as the reference.

Applying the same procedure (the semiempirical MO (PM5) method) as before, the AHT of the dyes on cellulose was analyzed by calculating the standard heat of formation for the two tautomers with the optimized structure in the gas phase and water. If one tautomer had higher stability in both phases, that tautomer was assumed to exist on cellulose as well. If different tautomers had higher stability in the two phases, both tautomers were assumed to possibly exist on cellulose.

For the tautomer(s) which may exist on cellulose, the electron densities in the HOMO and LUMO and the electrophilic frontier electron densities ($f_r^{(E)}$) in the gas phase were calculated by the PM5 method. The reactivity of a dye was determined as the sum ($S_{m,n}^{(E)}$, defined by Eq. (2)) of $f_r^{(E)}$ for the double bonds with potential reactivity against $^1O_2$. By calculating the heat of formation for the reaction intermediates and the end products of the reaction between the dye and $^1O_2$, the possible reaction modes were determined. Some reaction modes were excluded due to the excessive energy of formation.

By plotting $S_{m,n}^{(E)}$ value for the tautomer(s) of a dye against $\log k_0$ and carrying out the plotting for a series of dyes, a linear correlation line between $S_{m,n}^{(E)}$ and $\log k_0$ was obtained. The correlation lines for the azo dyes derived from γ-acid, J-acid and related naphthalene sulfonic acids had nearly the same slope, but were plotted at different positions in the graph.

The high reactivity of the azo dyes derived from γ-acid and 2R-acid in this series was attributed to the large values of $f_r^{(E)}$ and d_{HOMO} at C1 of the tautomers of Red 22 and to the stability of the corresponding tautomer on cellulose, while the low reactivity of the dyes in this series was attributed to the relatively small values of $f_r^{(E)}$ and d_{HOMO} at the potential double bonds of the HTs and to the high stability of the HTs on cellulose. These facts were predicted by frontier orbital theory and confirmed by the AHT analysis carried out using the MO method.

Quantitative structure–activity relationships (QSAR) and quantitative structure–property relationships (QSPR) were used with MO theory; they may prove useful or applicable in the research and development of new dyes.

Acknowledgement

This work was supported by a Grant-in-Aid for Scientific Research given by the Ministry of Education, Culture, Sports, Science and Technology of Japan.

References

[1] Rauk A. Orbital interaction theory of organic chemistry. 2nd ed. New York: Wiley-Interscience; 2001.
[2] Fleming I. Frontier orbitals and organic chemical reactions. New York: Wiley; 1976.
[3] Fukui K, Fujimoto H, editors. Frontier orbitals and reaction paths, selected papers of Fukui K, (World scientific series in 20th century chemistry vol. 7). Singapore: World Scientific; 1997.
[4] Kubinyi H. Quantitiative Structure–activity relationships in drug design. In: von R. Schleyer P, editor. Encyclopedia of computational chemistry, 4. Chichester: Wiley; 1998. p. 2309–20.
[5] Jurs PC. Quantitiative structure–property relationships (QSPR). In: von R. Schleyer P, editor. Encyclopedia of computational chemistry, 4. Chichester: Wiley; 1998. p. 2320–30.
[6] Karelson M. Molecular descriptors in QSAR/QSPR. New York: Wiley-Interscience; 2000.
[7] Morita Z, Hada S. A semiempirical molecular orbital study on the reaction of an aminopyrazolinyl azo dye with singlet molecular oxygen. Dyes and Pigments 1999;41(1):1–10.
[8] Hihara T, Okada Y, Morita Z. Reactivity of phenylazonaphthol sulfonates, their estimation by semiempirical molecular orbital PM5 method, and the relation between their reactivity and azo–hydrazone tautomerism. Dyes and Pigments 2003;59(3):201–22.
[9] Hihara T, Okada Y, Morita Z. Azo–hydrazone tautomerism of phenylazonaphthol sulfonates and their analysis using the semiempirical molecular orbital PM5 method. Dyes and Pigments 2003;59(1):25–41.
[10] Hihara T, Okada Y, Morita Z. Relationship between photochemical properties and colourfastness due to light-related effects on monoazo reactive dyes derived from H-acid, γ-acid, and related naphthalene sulfonic acids. Dyes and Pigments 2004;60(1):23–48.
[11] Hihara T, Okada Y, Morita Z. Photo-oxidation of pyrazolinylazo dyes and analysis of reactivity as azo and hydrazone tautomers using semiempirical molecular orbital PM5 method. Dyes and Pigments 2006; 69(2):151–76.
[12] Hihara T, Okada Y, Morita Z. Photo-oxidation of reactive azobenzene dyes and an analysis of reactivity as azo and hydrazone tautomers using PM5 method, submitted for publication.
[13] Okada Y, Hirose M, Kato T, Motomura H, Morita Z. Photofading of vinylsulfonyl reactive dyes on cellulose under wet conditions. Dyes and Pigments 1990;14(2):113–27.
[14] Okada Y, Hirose M, Kato T, Motomura H, Morita Z. Fading of vinylsulfonyl reactive dyes on cellulose in admixture under wet conditions. Dyes and Pigments 1990;14:265–85.
[15] Okada Y, Motomura H, Morita Z. Photosensitization and simultaneous reductive or oxidative fading of monochlorotriazinyl reactive dyes on cellulose under wet conditions. Dyes and Pigments 1992;20(2):123–35.
[16] Okada Y, Hirose M, Kato T, Motomura H, Morita Z. Catalytic fading of vinylsulfonyl reactive dye mixtures on cellulose under wet conditions. Dyes and Pigments 1990;12(3):197–211.
[17] Okada Y, Morita Z. Fading of some vinylsulfonyl reactive dyes on cellulose under various conditions. Dyes and Pigments 1992;18(4): 259–70.
[18] Okada Y, Kato T, Motomura H, Morita Z. Fading mechanism of reactive dyes on cellulose by simultaneous effects of light and perspiration. Sen'i Gakkaishi 1990;46(8):346–55.
[19] Okada Y, Motomura H, Morita Z. Simultaneous oxidative and reductive photofading of C.I. Reactive Red 22 and Black 5 on cellulose in presence of oxygen and substrate under wet conditions. Dyes and Pigments 1991;16(3):205–21.
[20] Okada Y, Orikasa K, Motomura H, Morita Z. Oxidative and reductive fading of monochlorotriazinyl reactive dyes on cellulose under wet conditions. Dyes and Pigments 1992;19(3):203–14.
[21] Lambert CR, Kochevar IE. Does Rose Bengal generate superoxide anion? Journal of the American Chemical Society 1996;118(13):3297–8.
[22] Bonnett R. Chemical aspects of photodynamic therapy. Amsterdam: Gordon and Breach Science Publishers; 2000.

[23] Byteva IM, Gurdzhiyan LM, Kaliya OL, Karpov VV, Korolev BA, Osmolovskaya LA, et al. Photodecomposition mechanism of reactive azo dyes in cellophane. Journal of General Chemistry of the USSR (Zhurnal Obshchei Khimii) 1991;61(12):2657–65.
[24] Foote CS, Clennan EL. Properties and reactions of singlet dioxygen. In: Foote CS, Valentine JS, Greenberg A, Liebman JF, editors. Active oxygen in chemistry. London: Blackie Academic & Professional; 1995. p. 105–40 [chapter 4].
[25] Frimer AA, Stephenson LM. The singlet oxygen ene reaction. In: Frimer AA, editor. Singlet O_2. Reaction modes and products, part 1, vol. 2. Boca Raton: CRC Press; 1985. p. 68–91 [chapter 3].
[26] Yamaguchi K. Theoretical calculations of singlet oxygen reactions. In: Frimer AA, editor. Singlet O_2. Reaction modes and products, part 2, vol. 3. Boca Raton: CRC Press; 1985. p. 119–251 [chapter 2].
[27] Kropf H, editor. Methoden der organischen chemie (Houben-Weyl), Band E.13, Teil 1 und 2, Organische peroxo-verbindungen. Stuttgart: George Thieme Verlag; 1988.
[28] Orfanopoulos M. Singlet oxygen ene-sensitizer photo-oxygenations: stereochemistry and mechanism. Molecular and Supramolecular Photochemistry 2001;8:243–85.
[29] Griesbeck AG, El-Idreesy TT, Adam W, Krebs O. Ene-reactions with singlet oxygen. In: Horspool WM, Lenci F, editors. CRC handbook of organic photochemistry and photobiology. 2nd ed. Boca Raton: CRC Press; 2003. p. 8-1–8-20 [chapter 8].
[30] Adam W, Beinhauer A, Hauer H. Activation parameters and excitation yields of 1,2-dioxetane chemiluminescence. In: Scaiano JC, editor. Handbook of organic photochemistry, vol. 2. Boca Raton: CRC Press; 1989. p. 271–327 [chapter 12].
[31] Fukui K, Yonezawa T, Shingu H. A molecular orbital theory of reactivity in aromatic hydrocarbons. Journal of Chemical Physics 1952;20(4):722–5.
[32] Fukui K, Yonezawa T, Nagata C, Shingu H. Molecular orbital theory of orientation in aromatic, heteroaromatic and other conjugated molecules. Journal of Chemical Physics 1954;22(8):1433–42.
[33] Fukui K, Yonezawa T, Nagata C. Interrelations of quantum-mechanical quantities concerning chemical reactivity of conjugated molecules. Journal of Chemical Physics 1957;26(4):831–41.
[34] CAChe Reference Guide [CAChe Reference Guide 4.9; 3-9–3-10], Fujitsu Ltd., 2002.
[35] Balgi S, Demir C. Identification of photooxidation degradation products of C.I. Reactive Orange 16 dye by gas chromatography–mass spectrometry. Dyes and Pigments 2005;66(1):69–76.